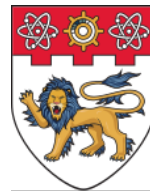


POLITECNICO DI TORINO

Corso di Laurea in Mechatronic Engineering

Tesi di Laurea Magistrale

Control design of an Uni-Drive module for elbow exosuit



Relatore
prof. Diego Regruto

Eugenio ANNESE
matricola: 220272

Supervisor
Nanyang Technological University
prof. Lorenzo Masia

ANNO ACCADEMICO 2017 – 2018

† Ai miei nonni

Summary

INTRODUCTION

A lot of different kind of exosuits were developed with different aims: restoring hand grasping, reducing metabolic cost of walking, assisting elbow movements. The main issue of these prototypes is that, most of time, reducing costs and weight implies to loose the possibility to actuate many degrees of freedom indipendently. The classical approach, derived from robotics, imposes to have one motor for each actuated DoF. It is evident that it is impossible in this case to save weight and money.

Other paths have been followed: articulated exosuits were designed, building kinematics and dynamics chains that with one motor actually moved many DoF but not indipendently.

A novel approach from robotics is winning these challenges: One-To-Many (or Uni-Drive) transmission. A One-To-Many transmission is a mechanical system that allows to tranfer motion from one power supply to many loads that work indipendently from each other: one power supply to many degrees of freedom.

This thesis starts from the work of Canesi in the Aries Lab of Nanyang Technological University under the supervision of Lorenzo Masia.

One To Many (OTM) Clutchable Exosuit: a novel prototype

Canesi developed a module for indipendent control of one DoF. The energy from power supply (prime mover, from here onwards) is trasferred to the module through a pinion gear, which meshes at orthogonally with two bevel gears facing each other: in this way gears will rotate in opposite directions. A passing countershaft is coupled with the rotor of two electro-mechanical clutches. The armature of clutches is coupled with their correspondent bevel gear. A third clutch is linked, on one side, to the countershaft, and on the other one to the frame. Coupled to the countershaft you can find a spool housing two cables wrapped in opposite directions used to transmit motion to the exosuit and, in particular, to the elbow joint. Cables work in typical muscle-like fashion: agonist/antagonist.

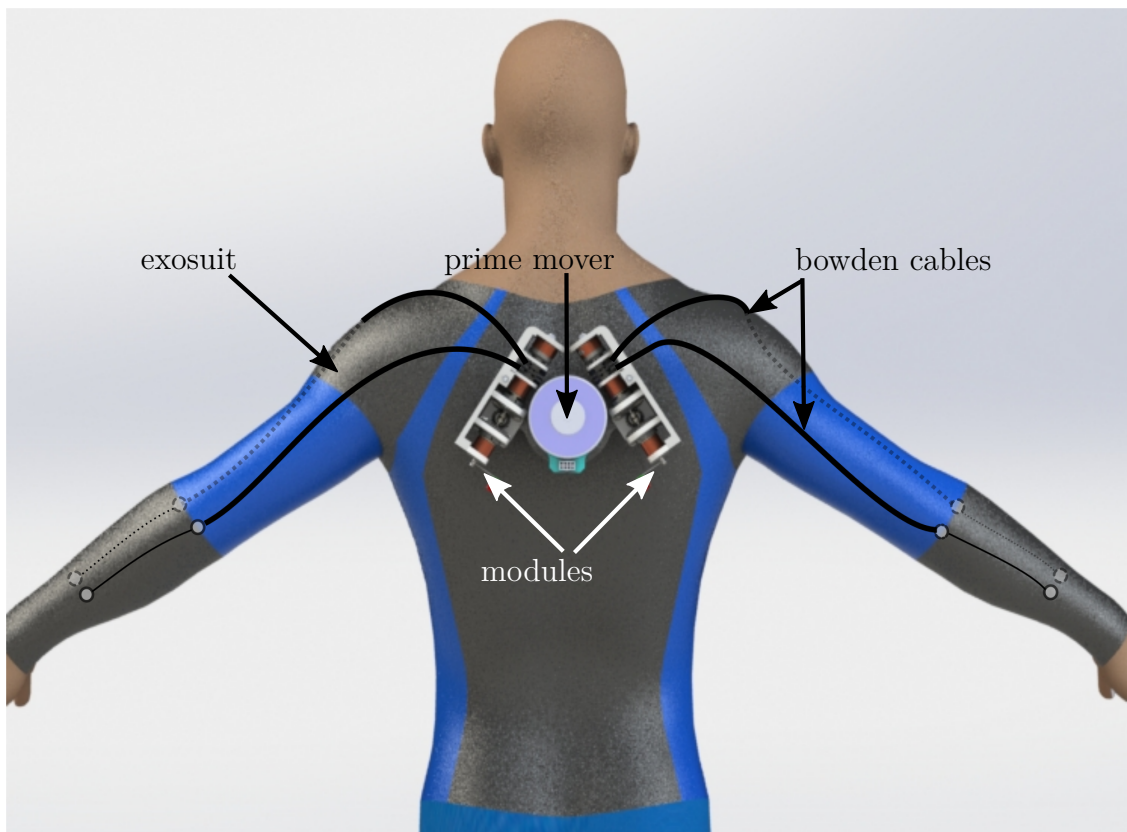


Figure 1: One To Many (OTM) mechanism for independently controlling two exosuits for the elbow. A single motor, referred to as *prime mover*, powers two modules, each independently driving one Degree of Freedom (DoF) via bowden cables.

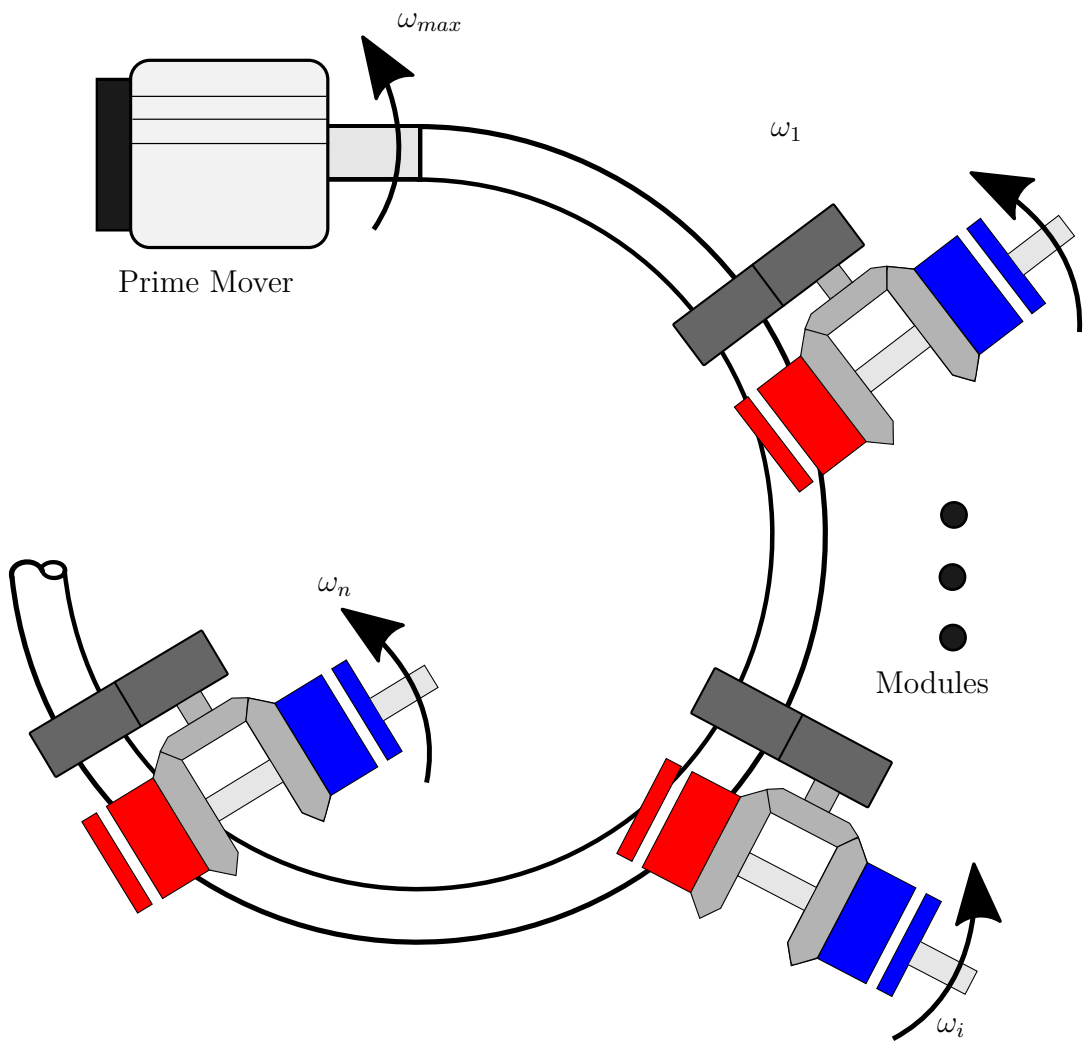


Figure 2: Schematics of the OTM paradigm

Working principle

The module works in 4 possible states:

1. **Free**, when all the clutches are disengaged, the output velocity at the pulley is not imposed by the prime mover and the wearer is free to move;
2. **Lock**, when the brake is engaged;
3. **Forward**, when the CW clutch is engaged, the output velocity equals the velocity of the prime mover divided by the reduction between the motor and the countershaft;
4. **Reverse**, when the CCW clutch is engaged, the output velocity equals the opposite velocity of the prime mover divided by the reduction between the motor and the countershaft.

The aim of this project is to upgrade mechanical design of the first prototype, propose a sliding mode approach for controlling the actuator and characterize it. Finally test on subject have been performed to evaluate the new module.

MECHANICAL DESIGN

The aim of these modifications is to improve mechanical robustness of the overall module, refine and balance mechanical behavior, compensate the discrete behavior of the output. In order to satisfy specifications, you can see a summary of main changes:

1. One main shaft;
2. New frame;
3. Substitution of clutch for reverse motion;
4. Adding a damper component between the main shaft and the output;
5. New spool for cable transmission.

Figure 3 shows a conceptual section of the new module.

Low level control architecture: PWM modulated by PID

The reference $r(t)$ for the controlled system is a trajectory θ_d that the spool has to follow, therefore the loop is closed in position. A PID stage modulates the error and is saturated between $[-1, +1]$ in order to give, as input for the PWM generator, a proper duty ratio.

In Figure 4 it is possible to visualise the actual control system. The thesis contains a particular section that describes the theoretical background of this approach: sliding mode regime.

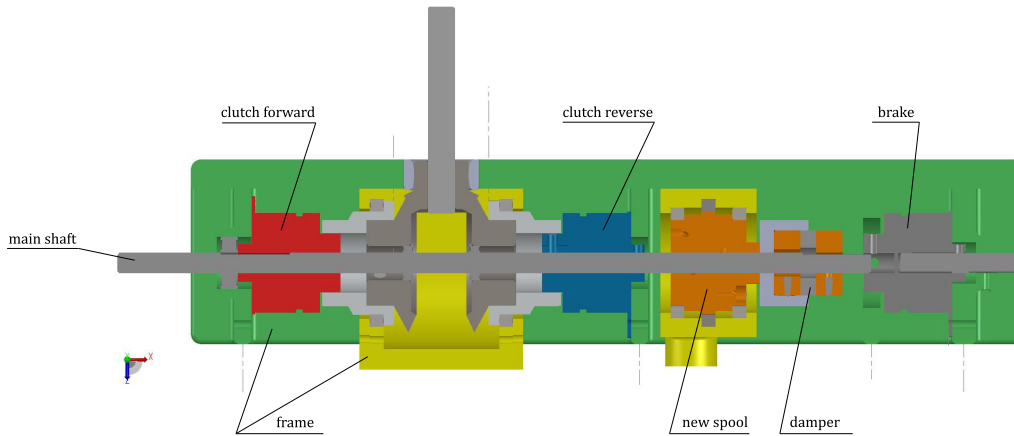


Figure 3: A conceptual section of the new module

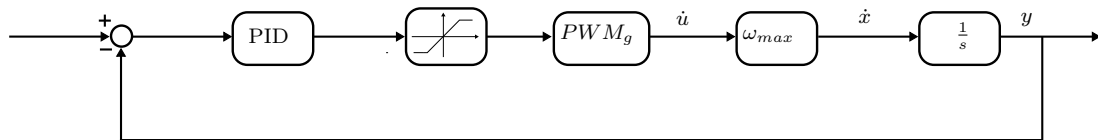


Figure 4: Schematics of the PID PWM control system

High level control: admittance control

The controller developed in this section is used to generate trajectories for the low-level controller. The aim of this control strategy is to assist users in elbow flexion/extension movements while compensating for the forearm's weight. The proposed controller is shown in Figure 5.

PERFORMANCE EVALUATION

Bandwidth

In Figure 6 are shown results of this test performed with different maximum velocities of the prime mover. From this graph it is possible to evaluate the cutoff frequency f_c of the system: when the amplitude is reduced by $-3dB$ (Table 3.2).

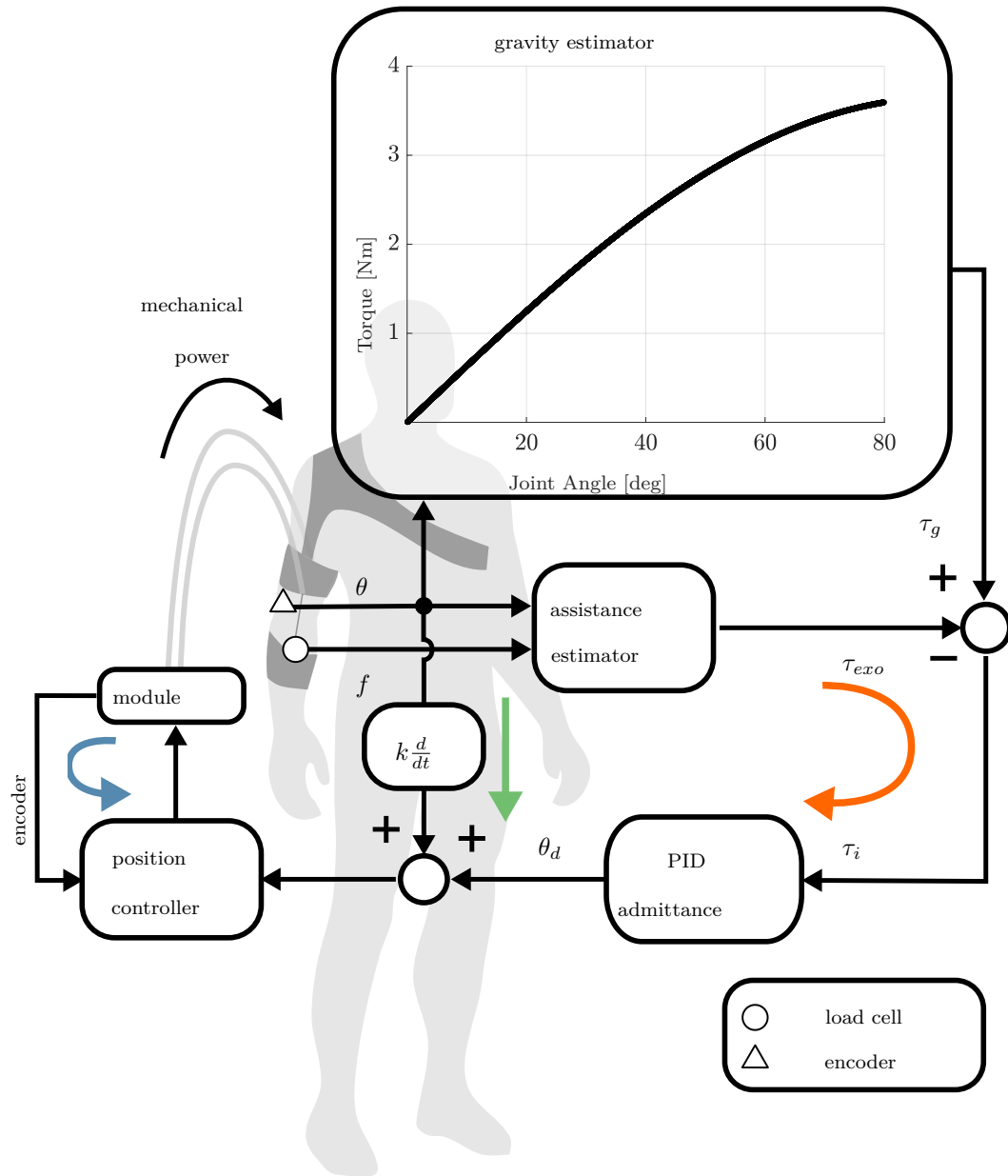


Figure 5: An outer torque loop (orange) tracks a reference profile equal and opposite to gravity, computing a motion reference as an interaction torque is sensed, according to the admittance specified by a PID controller. The low level control (light blue) is closed on the module position. The green arrow indicates a positive feedback path, introduced to improve transparency.

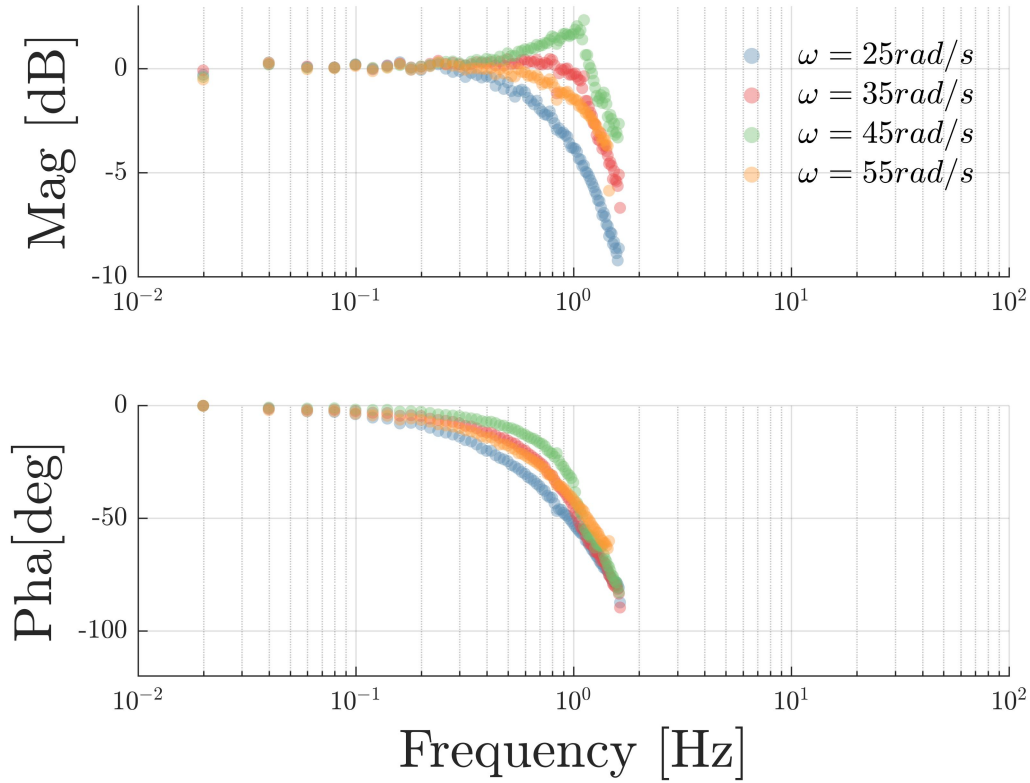


Figure 6: Bode diagrams at different values of ω_{max}

$\omega_{max} [rad/s]$	$f_c [Hz]$
25	0.88
35	1.26
45	1.51
55	1.30

Table 1: Cutoff frequencies for different values of ω_{max}

Loaded Behavior

The experiment consists in a set of different loads equally spaced from $0N$ to $11N$. The experiment was repeated 5 times. In Figure 7 are represented results of this analysis. We can say that the maximum cable's tension has to be lower than $8.2N$.

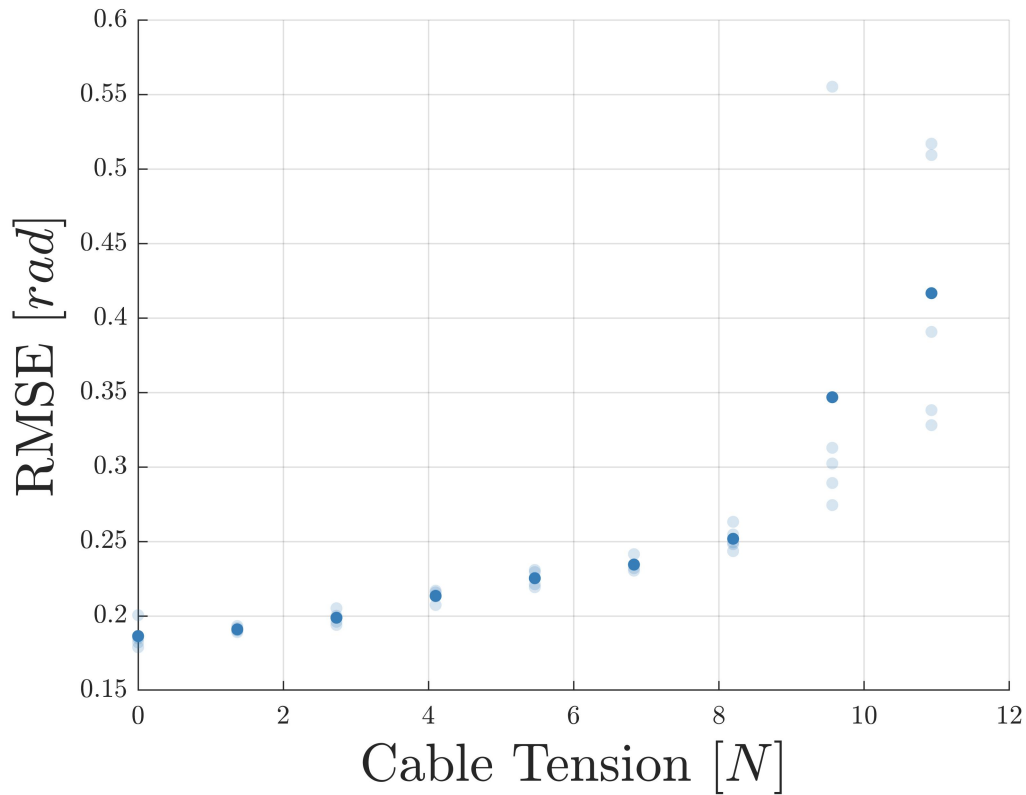


Figure 7: *RMSE* of the output position when the reference is a sine wave at constant frequency and cables are in tension with different loads

Test on subject

The experimental setup is shown in Figure 8. The reference motion consisted of series of Minimum Jerk Trajectories (MJT). In order to assess results from EMG analysis and trajectories we performed the same experiment using another actuator developed in the Aries Lab, called from here onwards DC module.

Muscular activity reduction

Muscular activity is represented quantitatively by the envelope EMG signal. In Figure 9 are shown EMG envelopes of the biceps during the experiment. Despite the fact the change with the module here described is just 30% compared with 55% of the DC module, it is a good result for a first prototype.

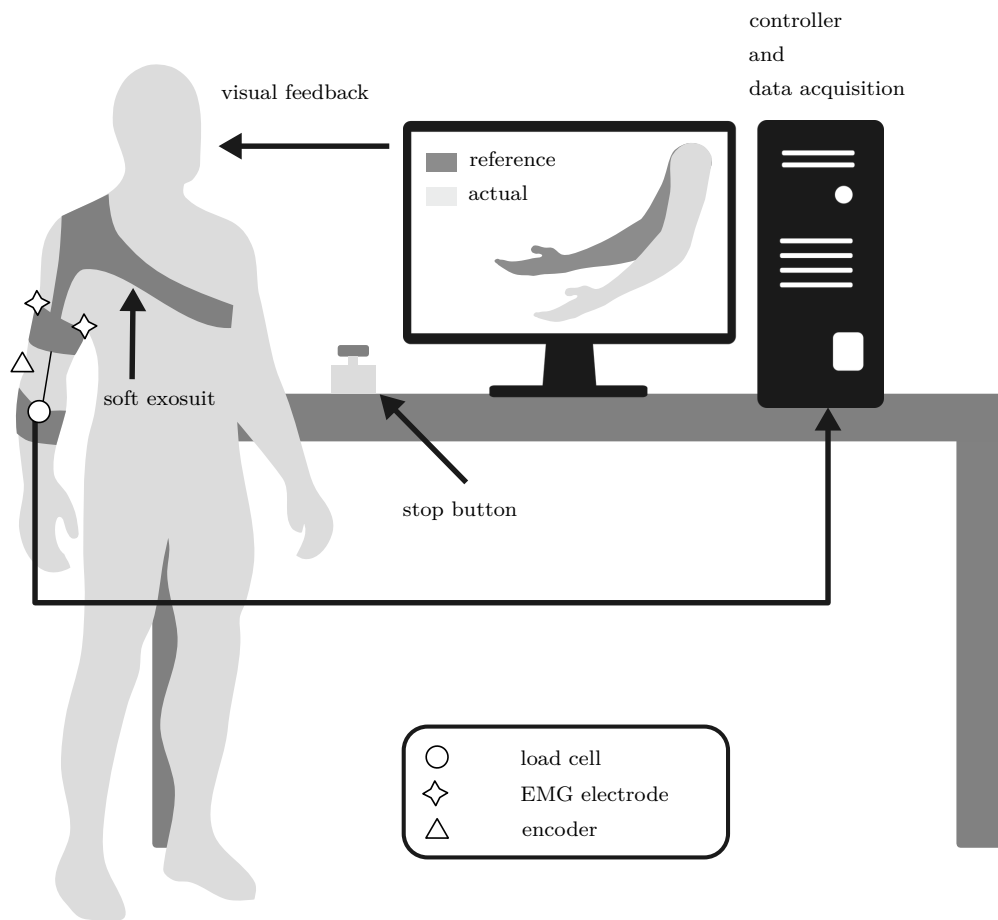


Figure 8: Experimental setup for tests on subject

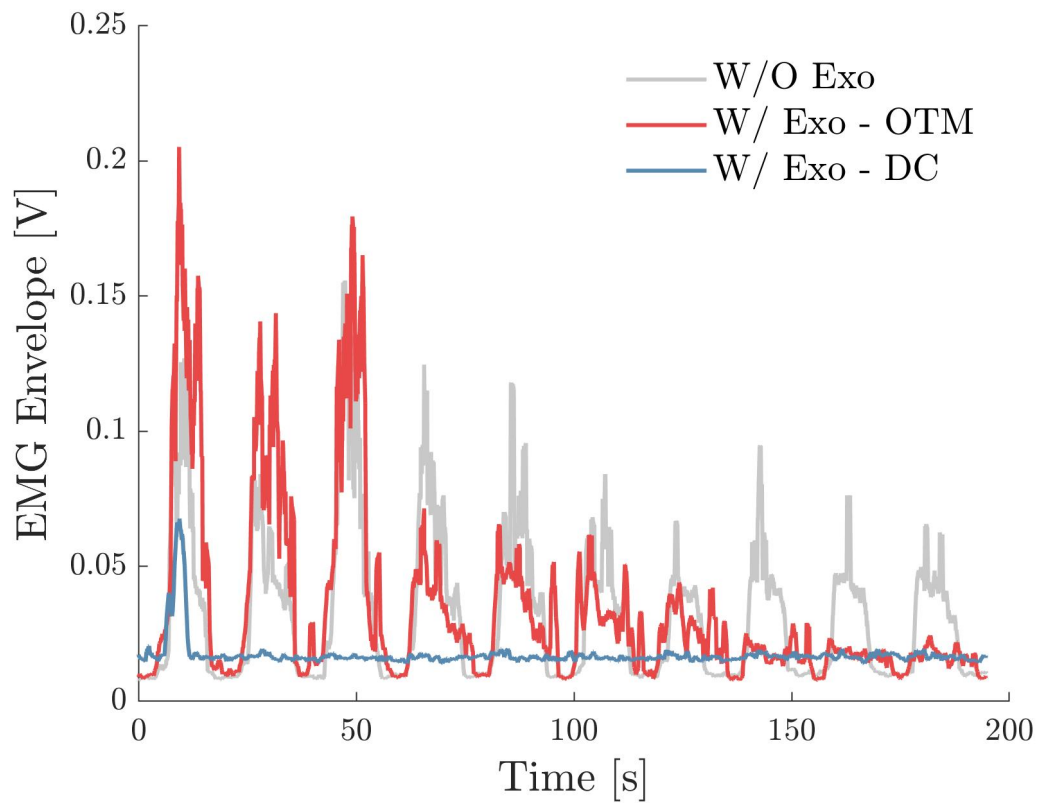


Figure 9: The envelope of the filtered absolute value of the EMG signal. In red the signal acquired using the OTM module, in blue using the DC motor prototype, in grey the without any assistance

Torque at the elbow joint analysis

In Figure 10 it is showed the torque distribution along one cycle between the subject (biological torque) and the exosuit. The overall torque that the subject has to produce is decreased by 45%.

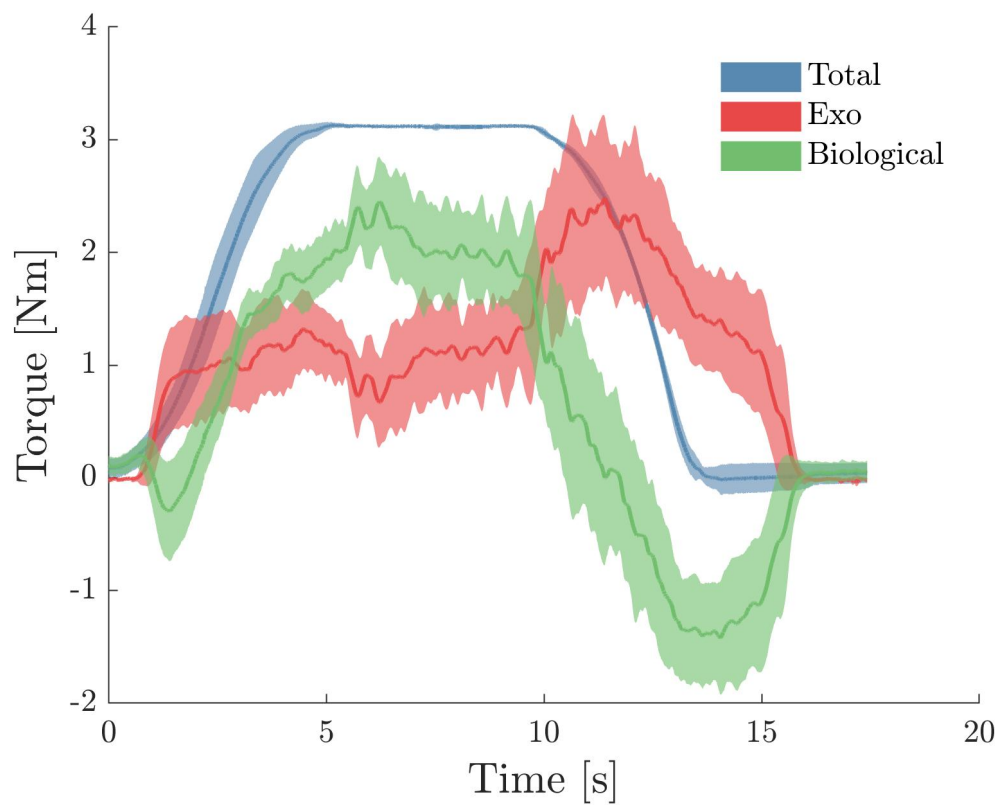


Figure 10: Requested torque average and standard deviation across all repetitions: in blue the total torque, in green the biological torque provided by the subject, in red the torque provided by the exosuit

Acknowledgements

I want to thank prof. Lorenzo Masia. He gave me the opportunity to work in his laboratory (Aries Lab) in NTU and this experience was so rich that this thesis is just a summary of what I lived there. But Lorenzo was also a mentor and a friend: I hope that everyone could find a supervisor like him.

I want to thank the PhD candidate Michele Xiloyannis. He helped in each phase of this work. The friendship born with him is a simple example of one point: becoming friends is possible when you are sharing a big project. The bigger the project is, the stronger the friendship would be.

The biggest contribution to this work belongs to my parents and my family. It is obvious and self-evident, but without each of them I could not do anything of what it is here described: they welcomed me into life. It is always worth to mention this contribution.

Finally, I want to thank my friends. They taught me that we can build a better world behaving like the water of a river: when it faces an obstacle, it will find a new path to reach the ocean. Thanks to Valentina: she is a promise fulfilled. You cannot do anything without a promise.

Contents

List of Tables	18
List of Figures	19
1 Introduction	23
1.1 Background	24
1.2 One To Many (OTM) Clutchable Exosuit: a novel prototype	26
1.2.1 Working principle	27
1.2.2 Main issues of the prototype	28
1.3 Aim of the Project	28
2 Materials and Methods	31
2.1 Exosuit Description	31
2.2 Mechanical Design	33
2.2.1 One main shaft	33
2.2.2 New frame	34
2.2.3 Substitution of clutch for reverse motion	35
2.2.4 Spool-damper transmission	35
2.3 ON-OFF-ON PWM Control Design	36
2.3.1 Theoretical Background	37
2.3.2 Saturation PWM controller	38
2.3.3 Clutches Engagement Time and Time Delay	38
2.4 Low level control architecture: PWM modulated by PID	40
2.4.1 PWM Generator	40
2.4.2 Logic Port	40
2.5 High level control: admittance control	42
2.5.1 PID Admittance control	43
2.6 Electro-mechanical hardware	46
2.6.1 DC motor	46
2.6.2 Clutches	46
2.7 Electronic control hardware	46
2.7.1 Test bench	47

2.7.2	Relays	49
2.8	Sensors	49
2.8.1	Shaft Encoder	50
2.8.2	Load Cell	50
2.8.3	Elbow Encoder	52
2.8.4	Surface EMG	52
3	Characterization and Performances Evaluation	53
3.1	Tuning Parameters	53
3.1.1	T_{PWM}	53
3.1.2	Tuning PID	55
3.2	Bandwidth	57
3.3	Loaded Behavior	61
3.4	Test on subject	62
3.4.1	Muscular activity reduction	63
3.4.2	Torque at the elbow joint analysis	66
4	Discussion and Future Works	73
4.1	Results	73
4.2	Discussion	74
4.3	Future works	74
	Bibliography	75
A	MATLAB codes	79
A.1	Choosing T_{PWM}	79
A.2	Trajectory tracking	80
A.3	Bandwidth	82
A.4	Load behavior	84
A.5	Test on subject	85

List of Tables

1	Cutoff frequencies for different values of ω_{max}	10
3.1	R^2 evaluated for curves of Figure 3.1	55
3.2	Cutoff frequencies for different values of ω_{max}	58

List of Figures

1	One To Many (OTM) mechanism for independently controlling two exosuits for the elbow. A single motor, referred to as <i>prime mover</i> , powers two modules, each independently driving one Degree of Freedom (DoF) via bowden cables.	5
2	Schematics of the OTM paradigm	6
3	A conceptual section of the new module	8
4	Schematics of the PID PWM control system	8
5	An outer torque loop (orange) tracks a reference profile equal and opposite to gravity, computing a motion reference as an interaction torque is sensed, according to the admittance specified by a PID controller. The low level control (light blue) is closed on the module position. The green arrow indicates a positive feedback path, introduced to improve transparency.	9
6	Bode diagrams at different values of ω_{max}	10
7	<i>RMSE</i> of the output position when the reference is a sine wave at constant frequency and cables are in tension with different loads	11
8	Experimental setup for tests on subject	12
9	The envelope of the filtered absolute value of the EMG signal. In red the signal acquired using the OTM module, in blue using the DC motor prototype, in grey the without any assistance	13
10	Requested torque average and standard deviation across all repetitions: in blue the total torque, in green the biological torque provided by the subject, in red the torque provided by the exosuit	14
1.1	Soft Wearable Assisting Devices for Hand, Lower and Upper Limb.	24
1.2	Schematics of the OTM paradigm	25
1.3	Front and back pictures of Canesi's OTM actuator, with 2 DoF	26
1.4	Schematics of the working principle of Canesi's actuator	27
1.5	Trapezoidal trajectory of the countershaft with the pinion rotating at a constant, unidirectional speed. Changing the pattern of activation of the clutches can be used to approximate any trajectory in a stepwise fashion.	28
2.1	Picture of the exosuit	32

2.2	A layout description of the exosuit's design. The exosuit comprises three straps that wrap around the shoulder, arm and forearm, highlighted in blue, orange and green, respectively. The last two act as anchor points: the Bowden cables' outer sheath is attached to the arm strap and the inner tendons to the forearm strap	33
2.3	A conceptual section of the new module	34
2.4	A side view of the main shaft	34
2.5	A 3D model of the frame	35
2.6	A conceptual section of the spool-damper transmission	36
2.7	An exploded view of the spool-damper transmission	36
2.8	Graph shows how engagement delay and friction affects output angular velocity	39
2.9	Schematics of the PID PWM control system	40
2.10	Schematics of the PWM Generator	42
2.11	Graphics summarizing the working principle of a PWM Generator, assuming a $T_{PWM} = 0.3s$	42
2.12	An outer torque loop (orange) tracks a reference profile equal and opposite to gravity, computing a motion reference as an interaction torque is sensed, according to the admittance specified by a PID controller. The low level control (light blue) is closed on the module position. The green arrow indicates a positive feedback path, introduced to improve transparency.	44
2.13	Routing of the tendons along the elbow exosuit	45
2.14	Picture of the DC motor	47
2.15	Picture of the electromechanical clutch from catalogue	47
2.16	Picture of the Quanser QPIDE	48
2.17	Connections layout of EPOS2 50/5 from catalogue	49
2.18	Picture of the relay module	50
2.19	Schematic of a single Module of the Relay	51
2.20	A picture of the load cell	51
2.21	Drawing of the encoder from catalogue	52
3.1	Duty Ratio effect at different T_{PWM}	54
3.2	Experimental setup for evaluating ramp trajectory tracking. The reference is a ramp with slope ω that is a fraction of ω_{max} . Low level control produces an input u for the logic port that sends commands to clutches.	56
3.3	A sample of I/O response of the system when the reference is a ramp. In this case $\omega_{max} = 45rad/s$	57
3.4	The influence of ω_{max} on tracking performance of the actuator: evaluated by $RMSE$ of the output position and ramp references with slopes fractions of the maximum velocity	58

3.5	Experimental setup for evaluating ramp trajectory tracking. The reference is a ramp with slope ω that is a fraction of ω_{max} . Low level control produces an input u for the logic port that sends commands to clutches.	59
3.6	A sample of I/O response when the reference is a sine wave	60
3.7	Bode diagrams at different values of ω_{max}	61
3.8	Experimental setup for evaluating loaded behavior of the module. The reference is a sine wave with amplitude correspondent to $90deg$. Load is imposed in the sense of cables' tension through driving the second motor in current.	62
3.9	<i>RMSE</i> of the output position when the reference is a sine wave at constant frequency and cables are in tension with different loads . .	63
3.10	Experimental setup for tests on subject	64
3.11	Experimental trajectories datasets collected from the elbow encoder in three conditions: in red data acquired using the OTM module, in blue using the DC motor prototype, in grey without any assistance	65
3.12	Raw EMG signal as acquired. In red the signal acquired using the OTM module, in blue using the DC motor prototype, in grey without any assistance	66
3.13	The envelope of the filtered absolute value of the EMG signal. In red the signal acquired using the OTM module, in blue using the DC motor prototype, in grey without any assistance	67
3.14	Perceptual reduction of muscular activity. In red the signal acquired using the OTM module, in blue using the DC motor prototype, in grey without any assistance	68
3.15	Requested torque mean and standard deviation across repetitions: in blue the total torque, in green the biological torque provided by the subject, in red the torque provided by the exosuit	69
3.16	Distribution of the total torque between subject and exosuit.	70
3.17	Perceptual reduction of human effort in terms of torque using the exosuit.	71

*Non è suo moto per altro distinto,
ma li altri son misurati da questo,
sì come diece da mezzo e da quinto.*
[D. ALIGHIERI, *Divina Commedia*,
Paradiso, XXVII, 106-117]

Chapter 1

Introduction

In the last few decades a great effort has been put in order to develop novel exoskeletons as assistive technologies. Despite the fact that the first application of this device was teleoperation [2] nowadays we can observe a lot of different applications: power enhancement in industry [3], assistive technology in neurorehabilitation of extremities[4]. Although earlier prototypes were rigid, complex, heavy and fully powered focus of last researchs is on soft, wearable devices.

The main reason of this change of paradigm was the need of reducing costs and amplify portability during daily tasks such as working in factory or, simply, fulfill normal activities, i.e. lifting a glass of water.

It is worth to underline that impairments after strokes or due to ageing are spreading up in last decades [1]. This results in an increasing need of new technologies that combine power augmentation and full wearability.

A lot of different kind of exosuits were developed with different aims: restoring hand grasping¹ [5][6][7][9], reducing metabolic cost of walking² [10][11], assisting elbow movements³[12][13][14].

The main issue of these prototypes is that, most of time, reducing costs and weight implies to loose the possibility to actuate many degrees of freedom independently. The classical approach, derived from robotics, imposes to have one motor for each actuated DoF. It is evident that it is impossible in this case to save weight and money.

Other paths have been followed: articulated exosuits were designed, building kinematics and dynamics chains that with one motor actually moved many DoF but not independently[6][8].

It is clear now that a great effort is needed to develop novel actuators: smaller,

¹Image Source: <http://biorobotics.snu.ac.kr/research/ckattempt=1>

²Image Source: <https://wyss.harvard.edu>

³Image Source: <https://lorenzomasia.info/projects>

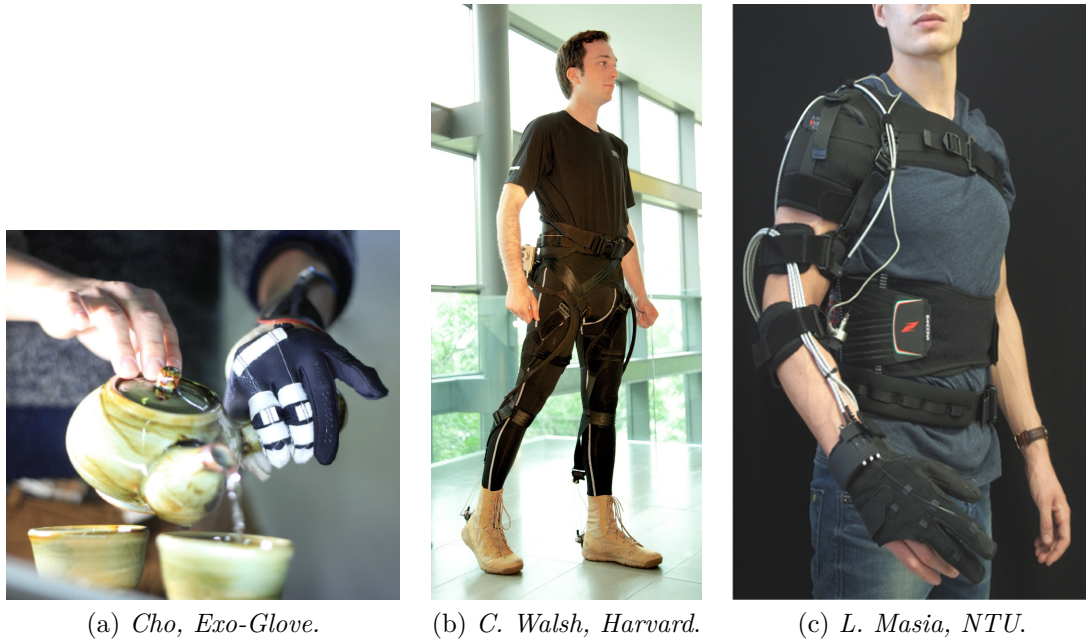


Figure 1.1: Soft Wearable Assisting Devices for Hand, Lower and Upper Limb.

low-cost, backdrivable and controllable as needed. A novel approach from robotics is winning these challenges: One-To-Many (or Uni-Drive) transmission.

1.1 Background

A One-To-Many transmission is a mechanical system that allows to transfer motion from one power supply to many loads (module) that work independently each other: one power supply to many degrees of freedom. This idea is ancient. The Greek philosopher Aristotele (4th century B.C.) described the physics of the world assuming the divinity as a source of an infinite power motion that transmits its energy to everything. Dante Alighieri in his masterpiece *La Divina Commedia* (1320 A.D.), using the same image of Aristotele described the astronomy of the universe. Alighieri imagined a first sky that receives God's energy and transfers it through its motion to lower skies that rotate at a speed that is a fraction of the first one:

*Non è suo moto per altro distinto,
ma li altri son misurati da questo,
sì come diece da mezzo e da quinto.*

[D. ALIGHIERI, *Divina Commedia*, Paradiso, XXVII, 106-117]

Engineering technology takes often inspiration from nature's observation, more

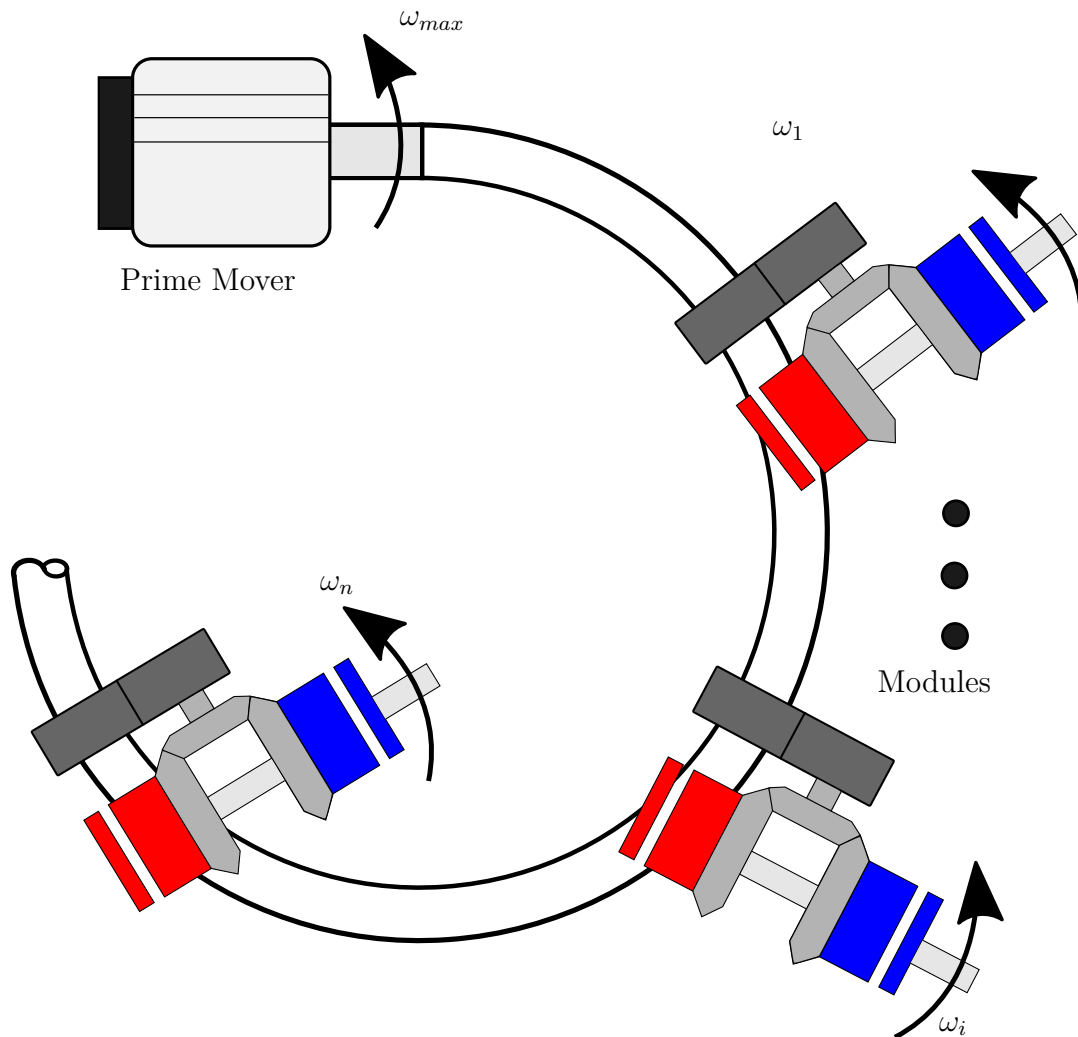


Figure 1.2: Schematics of the OTM paradigm

rarely from philosophy: this is a singular exception.

The One-To-Many concept in engineering has many meanings and applications. For example, in database One-To-Many describes a class of relations. Introducing OTM in a mechatronic context implies to answer to one question: is it possible to transfer motion from one motor to many actuators independently? Then, if the answer is yes, how? This question is so capital, in fact, answering yes would let us say with Karbasi[28]:

Unidrive modular robots because of employing only a single drive for operating all joints have a substantial advantage over regular modular robots in terms of the mass of each module. The drive is mounted at the robot base and all joints tap power from the single drive using clutches.

The main path followed by scientists to answer the question is using clutches, in the most of the case electromechanical ones. If the main motion of the prime mover could be fractioned, each joint would be independent: it is the same image of Alighieri's astronomy. Popovic described these systems as a mechanical equivalent of hydraulic or pneumatic system. In fact, motor acts as a pump and clutches as fluid valves. Now, one can imagine how much wide is the potential of this paradigm. In the last decade a lot of novel designs have been developed under the One-To-Many paradigm due to its intrinsic flexible nature. Xie [19] designed a robotic manipulator, Tirasuntarakul [18] a controller for a Thai hammered dulcimer, Jia [17] a robotics dexterous hand.

The exploration of OTM architectures involved scientists not just on different kind of applications. In fact, this paradigm has been improved. Popovic [15] inserted series elastic components between power source and modules in order to optimise energy consumption. Penn [16] designed an actuator with a vibrating transducer on parallel network of resonator. Another way to transfer power could be IVT: the work of Kernbaum [29] is a suitable solution for all issue described above. In fact, the effort of designing actuators for Uni-drive systems was focused on clutches. The possibility of using an IVT is a compact, light and efficient alternative. IVT could introduce a smoother velocity driver for controlling modules. This thesis focuses on the work of Canesi [24] in the Aries Lab of Nanyang Technological University under the supervision of Lorenzo Masia.

1.2 One To Many (OTM) Clutchable Exosuit: a novel prototype

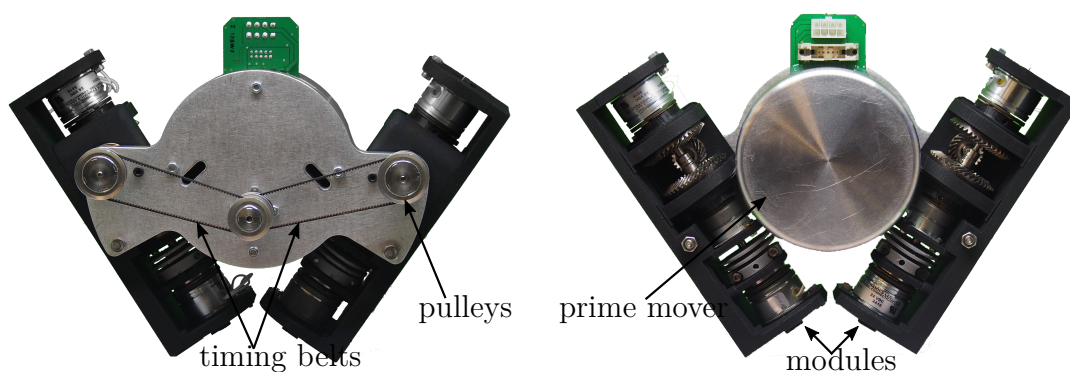


Figure 1.3: Front and back pictures of Canesi's OTM actuator, with 2 DoF

Canesi developed a module for independent control of one DoF. The energy from a single mechanical power supply (prime mover, from here onwards) is transferred

to the module through a pinion gear, which meshes orthogonally with two bevel gears facing each other: in this way the gears will rotate in opposite directions. A passing countershaft is coupled with the rotor of two electro-mechanical clutches. The armature of the clutches is coupled with their correspondent bevel gear. A third clutch is linked, on one side, to the countershaft, and on the other one to the frame. Coupled to the countershaft you can find a spool housing two cables wrapped in opposite directions used to transmit motion to the exosuit and, in particular, to the elbow joint. Cables work in typical muscle-like fashion: agonist/antagonist.

1.2.1 Working principle

The module works in 4 possible states:

1. **Free**, when all the clutches are disengaged, the output velocity at the pulley is not imposed by the prime mover and the wearer is free to move;
2. **Lock**, when the brake is engaged;
3. **Forward**, when the CW clutch is engaged, the output velocity equals the velocity of the prime mover divided by the reduction between the motor and the countershaft;
4. **Reverse**, when the CCW clutch is engaged, the output velocity equals the opposite velocity of the prime mover divided by the reduction between the motor and the countershaft.

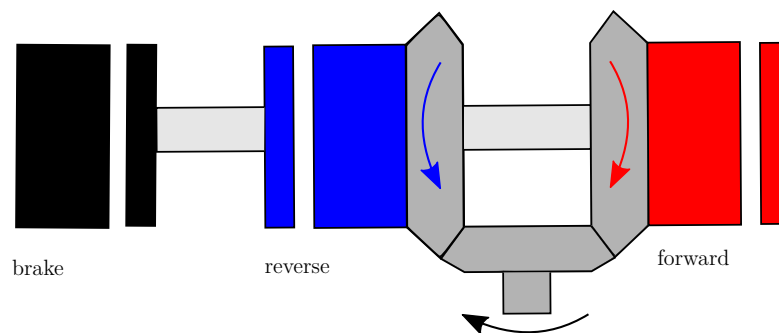


Figure 1.4: Schematics of the working principle of Canesi's actuator

The control scheme, implemented on this first design, was a finite state machine. The idea is simple and it is based on the fact that the system can shift just between states described above. The control law works by checking the error and its derivative and choosing if holding the present state or shifting toward another to minimize the error between a desired and measured trajectory.

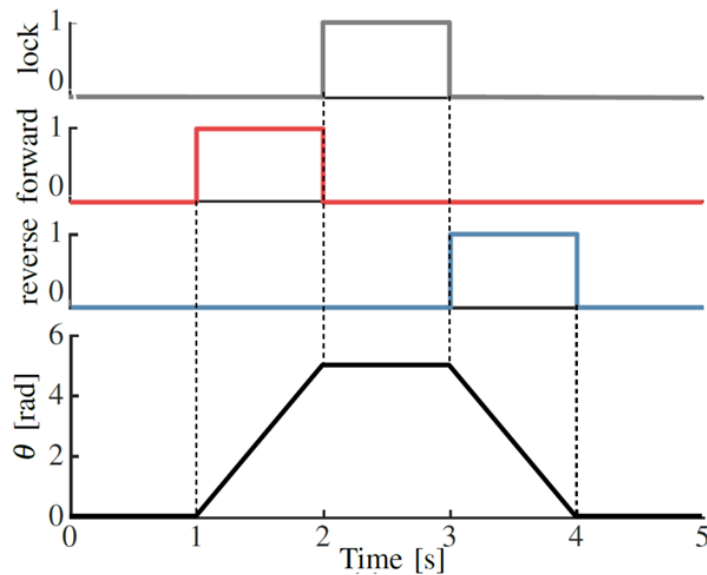


Figure 1.5: Trapezoidal trajectory of the countershaft with the pinion rotating at a constant, unidirectional speed. Changing the pattern of activation of the clutches can be used to approximate any trajectory in a stepwise fashion.

1.2.2 Main issues of the prototype

Because of the starting point of this work is this first design it is worth to underline what are main problems of this first architecture.

From a mechanical point of view we observed that the output trajectory were twitching: this is a serious issue when using this actuator to assist human movements. Furthermore, from a structural point of view, the frame of each module results to be not rigid enough, and forces tend to deformate periodically the entire structure.

The control approach, although effective, was lacking of robustness becoming unstable when excited with strong perturbations.

1.3 Aim of the Project

The aim of this project is to upgrade the mechanical design of the first prototype, propose a sliding mode approach for controlling the actuator and characterize it. Next chapters describe:

- materials and methods utilised with a particular focus on theoretical background under control architecture;

- characterization of the actuator and evaluation of performances when exosuit is used by a subject;
- discussion about results and definition of future works.

Chapter 2

Materials and Methods

2.1 Exosuit Description

An exosuit is a device consisting of a frame made of soft material that wraps around the human body and transmits forces to its wearer's skeletal structure. In a cable-driven exosuit, artificial tendons are routed along a targeted joint and attached to anchor points on both of its sides. When the tendons are tensioned they deliver an assistive moment to the joint. The exosuit for assistance of the elbow joint presented in this thesis (shown in Figures 2.1 and 2.2) follows exactly this principle.

It comprises of three fabric straps: one around the forearm (distal anchor point), one around the arm (proximal anchor point) and a shoulder harness, connected to the arm strap via adjustable webbing bands. Buckles, velcro straps and a Boa lacing system allow to tighten the suit. A pair of Bowden cables transmits power from an actuation unit to the anchor points. The Bowden cables sheaths (Shimano SLR, 5 mm) are attached to the arm strap, while their inner tendons (Dupont, Black Kevlar Fiber, 136 kg max load) to the forearm strap. When either of the two tendons is shortened, it pulls together the two anchor points, applying a flexing or extending moment on the elbow.

The shoulder harness is connected via inextensible webbing bands to the arm strap, covers the shoulder and encircles the chest; its purpose is to prevent the arm strap from migrating towards the center of the joint by relying on reaction forces from the shoulder and ribcage. The same is achieved for the forearm strap by tightening it with a boa lacing system, the conic shape of the forearm contributes to prevent slippage.

The proximal and chest straps were made by modifying a commercially available passive orthosis (Master-03, Reh4mat). Their substrate is made of a 3-layered fabric: an external layer used to attach hard components (buckles and webbing strips), an intermediate ethylene-vinyl acetate (EVA) foam to avoid peaks of pressure and an internal 3D polyamid structure to provide air permeability. The distal anchor point consists of a flexible plastic sheet, lined with ballistic nylon and covered by



Figure 2.1: Picture of the exosuit

a 3 mm-thick layer of polyethylene (PE) sponge at the interface with the skin. A load cell, secured on the distal anchor point, measures the tension in the flexing tendon and an absolute encoder, mounted on a 3D-printed joint (Shapeways, versatile plastic) between the arm and forearm straps, senses the angular position of the elbow.

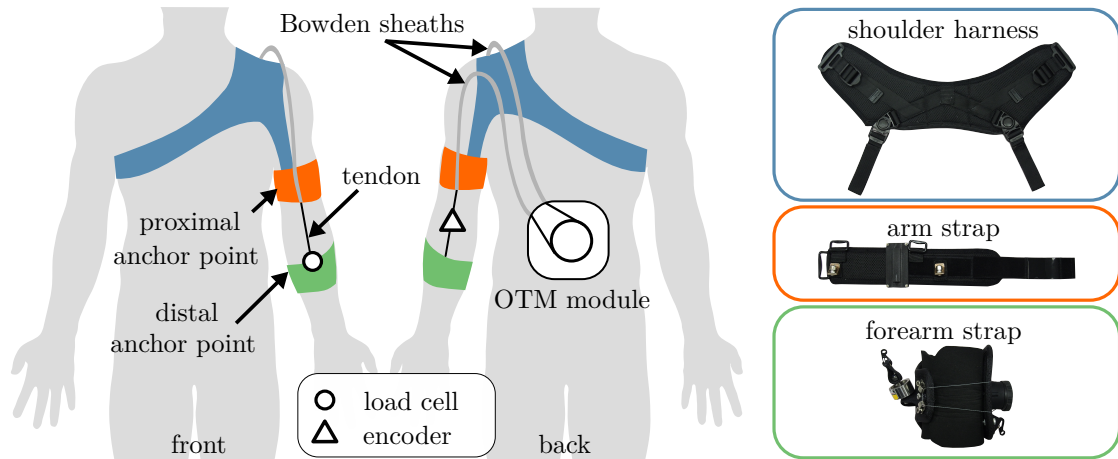


Figure 2.2: A layout description of the exosuit's design. The exosuit comprises three straps that wrap around the shoulder, arm and forearm, highlighted in blue, orange and green, respectively. The last two act as anchor points: the Bowden cables' outer sheath is attached to the arm strap and the inner tendons to the forearm strap

2.2 Mechanical Design

In this section it is explained what are the main improvements of the novel actuator. In particular, the aim of these modifications is to improve mechanical robustness of the overall module, refine and balance mechanical behavior and compensate for the discrete behavior of the output. In order to satisfy specifications, you can see a summary of main changes:

1. One main shaft;
2. New frame;
3. Substitution of clutch for reverse motion;
4. Adding a damper component between the main shaft and the output;
5. New spool for cable transmission.

In 2.3 it is showed a conceptual section of the new module.

2.2.1 One main shaft

The old module had 2 shafts coupled in correspondence of the differential transmission. This solution generated two problems:

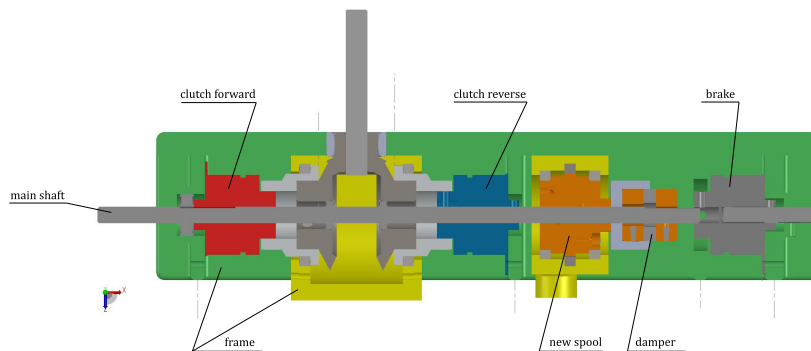


Figure 2.3: A conceptual section of the new module

1. The need of a section reduction to couple shafts: from 6mm to 4mm that results in unneeded increasing of the stress along shafts during operations.
2. The small coupling between shafts was expensive and connected by small set-screw and not rated to hold the torque required for this application.

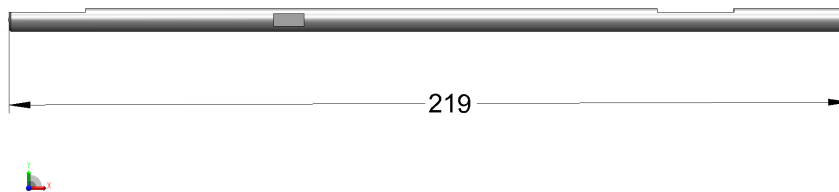


Figure 2.4: A side view of the main shaft

The simplest solution was to design a single shaft with flat insertions in the right places for clutches and the spool-damper system. In 2.4 there is a side view of the new design.

2.2.2 New frame

Rigidity of the frame is a crucial aspect of the mechanical design. In fact, the high forces have to be balanced by the frame to guarantee a continuous transmission. The frame of old prototype, after many cycles, started to plastically deformate in correspondence of the differential transmission. The reason is that gears generate

axial force that try to turn away the two gears from the pinion. The solution for this problem was to augment the material quantity of the frame. To balance axial forces screws linking walls to main frame are added near to the gears on the main frame. In figure 2.5 you can see a 3D model of the new frame and, in blue, the cage with places for screws.

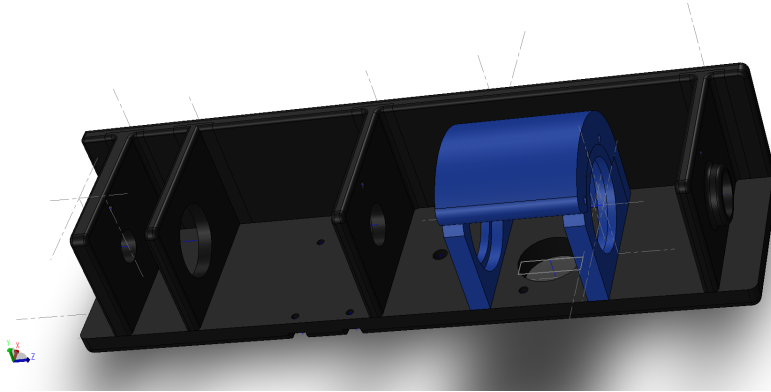


Figure 2.5: A 3D model of the frame

2.2.3 Substitution of clutch for reverse motion

Another issue of the old prototype was that one clutch was different from the other two. As we will discuss in 2.3 clutches generate some phenomena that modify control requirements and the simmetry of the system is a condition for stability. Thus, in particular in loaded conditions, different clutches result in an asymmetric behavior of the control system. Therefore we substituted the clutch for reverse motion with one identical to the other two.

2.2.4 Spool-damper transmission

This module, by principle, works changing state every T_{PWM} (see 2.3). Each state imposes a different velocity and acts like a step. Thus the output behavior is scattered around the desired position. To limitate this uncomfortable consequence we added a damper between the main shaft and the spool. The damper is a coupling that on one side is linked with the main shaft and, on the other side through screws to the spool. The new spool is designed like a cage for cables. In fact, in different condition of motion cables are not always in tension. This is a problem and the risk is that, without a cage, they can go out of their place and interrupt the trasmission of motion. In figures 2.6 and 2.7 it is shown this transimission system, respectively in section and exploded view.

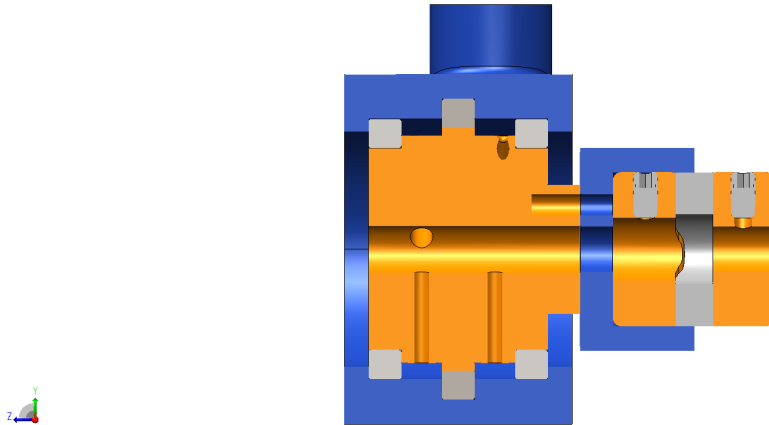


Figure 2.6: A conceptual section of the spool-damper transmission

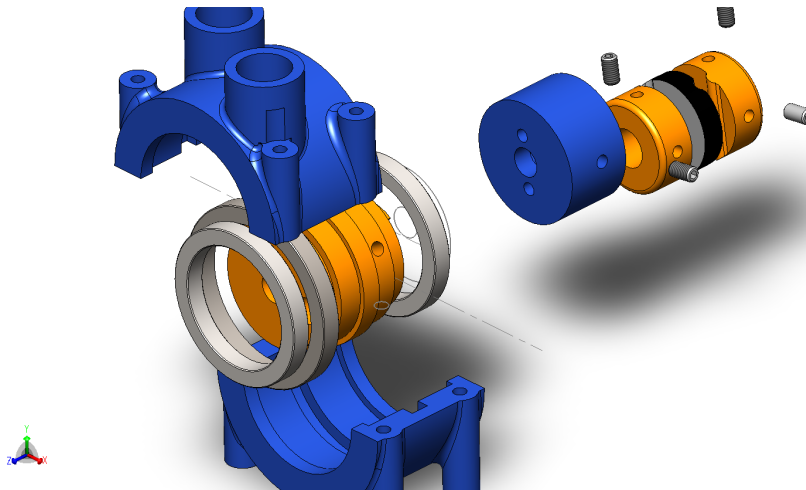


Figure 2.7: An exploded view of the spool-damper transmission

2.3 ON-OFF-ON PWM Control Design

The system working principle shows that the actuator has 3 working states: forward, reverse and brake. The first approach to control this system was a state-machine, described in [24]. We are proposing a different approach: an ON-OFF-ON Pulse Width Modulation.

Karbasi [23] proposed this kind of control on a similar system. The main idea is that the behaviour of a non-linear system is the same of the average model, under certain conditions. In the next sections you can find the theoretical approach to the ideal system and then the experimental procedure to evaluate proper parameters for the PWM controller.

2.3.1 Theoretical Background

Let consider an ideal nonlinear PWM controlled system that behaves like the actual one we are studying

$$\begin{cases} \frac{dx}{dt} = u(t)\omega_{max} \\ y(t) = x(t) \\ e(t) = r(t) - y(t) \\ u(t) = PWM_{\tau}[e(t_k)] \end{cases}$$

where

1. $u(t)$ is the control signal such that $u(t) \in \{-1,0,1\}$: it is the ON-OFF-ON input;
2. $x(t)$, the state variable.
3. $e(t)$ is the error between the reference $r(t)$ and the output $y(t)$
4. ω_{max} is the angular velocity of the shaft $[\omega_{max}] = \text{rad/s}$;
5. t_k represents regularly spaced instants of time where an ideal sampling process takes place;
6. $PWM_{\tau}[e(t_k)]$ the PWM control operator, usually characterized as follows (see [20])

$$PWM_{\tau} = \begin{cases} \text{sgn}[e(t_k)] & \text{for } t_k \leq t \leq t_k + \tau[e(t_k)]T_{PWM} \\ 0 & \text{elsewhere} \end{cases}$$

It is possible to consider a set of instants T_i such that $x(t) \geq 0$ or $x(t) \leq 0$ if $t \in (T_i - 1; T_i)$. Without loss of generality we can assume that these intervals are such that $T_{PWM} \gg T_i$. Let suppose that $t \in (T_i - 1; T_i)$, in this interval we can compute the average time derivative of $x(t)$ when T_{PWM} tends to 0:

$$\left(\frac{dx}{dt}\right)_{avg} = \lim_{T_{PWM} \rightarrow 0} \frac{x(t_k + T_{PWM}) - x(t_k)}{T_{PWM}}$$

In order to evaluate this limit we have to compute

$$x(t_k + T_{PWM}) = x(t_k) + \int_{t_k}^{t_k + \tau[e(t_k)]T_{PWM}} \omega_{max} dt = x(t_k) + \omega_{max} \tau[e(t_k)] T_{PWM} \text{sgn}[e(t_k)]$$

If $T_{PWM} \rightarrow 0$, $t_k \rightarrow t$. Thus the average velocity is:

$$\left(\frac{dx}{dt}\right)_{avg} = \omega_{max} \tau[e(t)] \text{sgn}[e(t)]$$

We obtained an average model that behaves like the sampled one under the condition of operating at a sufficiently small T_{PWM} . Before to discuss about choosing the frequency of the controller we need a suitable duty ratio function.

2.3.2 Saturation PWM controller

It is needed to choose a proper duty ratio function $\tau[e(t_k)]$ that has to be a smooth function of even nature. As you can see in [21] a good choice is the so called saturation function of the error signal:

$$\tau[e(t_k)] = \begin{cases} \beta|e(t_k)| & \text{for } |e(t_k)| \leq 1/\beta \\ 1 & \text{for } |e(t_k)| > 1/\beta \end{cases}$$

Calling $N[e(t_k)]$ the odd function:

$$N[e(t_k)] = \tau[e(t_k)]\text{sgn}(e(t_k))$$

You can see that the average block substituting the PWM controller is given by

$$N[e(t)] = \tau[e(t)]\text{sgn}(e(t)) = \text{sat}[e(t)]$$

The nature of the actual PWM controller is that the state responses coincide in the saturation region $|e(t)| > 1/\beta$. In the boundary region state responses slide about integral manifolds of the average system (See [22]). Now we have a control architecture that assures stability for the system. In summary, the the controlled system is described by the following equations during the sampling process:

$$\begin{cases} \frac{dx}{dt} = u(t)\omega_{max} \\ y(t) = x(t) \\ e(t) = r(t) - y(t) \\ u(t) = PWM_{\tau}[e(t)] \end{cases}$$

and

$$PWM_{\tau} = \begin{cases} \text{sgn}[e(t_k)] & \text{for } t_k \leq t \leq t_k + \tau[e(t_k)]T_{PWM} \\ 0 & \text{elsewhere} \end{cases}$$

With $\tau[e(t_k)]$ defined as we stated earlier.

2.3.3 Clutches Engagement Time and Time Delay

The main difference between the ideal system and the actual one is the time delay due to engagement and disengagement of clutches. SWC have an engagement time and a control strategy needs to take into account this phenomenon. Karbasi [23] modelled the phenomenon with an engagement delay δ to reach desired velocity ω_d and at disengagement with the delay and a friction that decreases exponentially in time. In figure 2.8 you can see the velocity output due to generic command u

from PWM Generator. Therefore it is possible to estimate the average velocity as follows

$$\omega_d = \frac{dy}{dt} = \frac{1}{T_{PWM}} \left[\omega_{max}(\tau[e(t_k)]T_{PWM} - \delta) + \int_0^{T_{PWM} - \tau[e(t_k)]T_{PWM} + \delta} \omega_{max} e^{-\frac{c}{I}t} dt \right]$$

where

1. c is the angular damping [c] = N m s rad⁻¹
2. I is the moment of inertia of the rotor [I] = kg m²

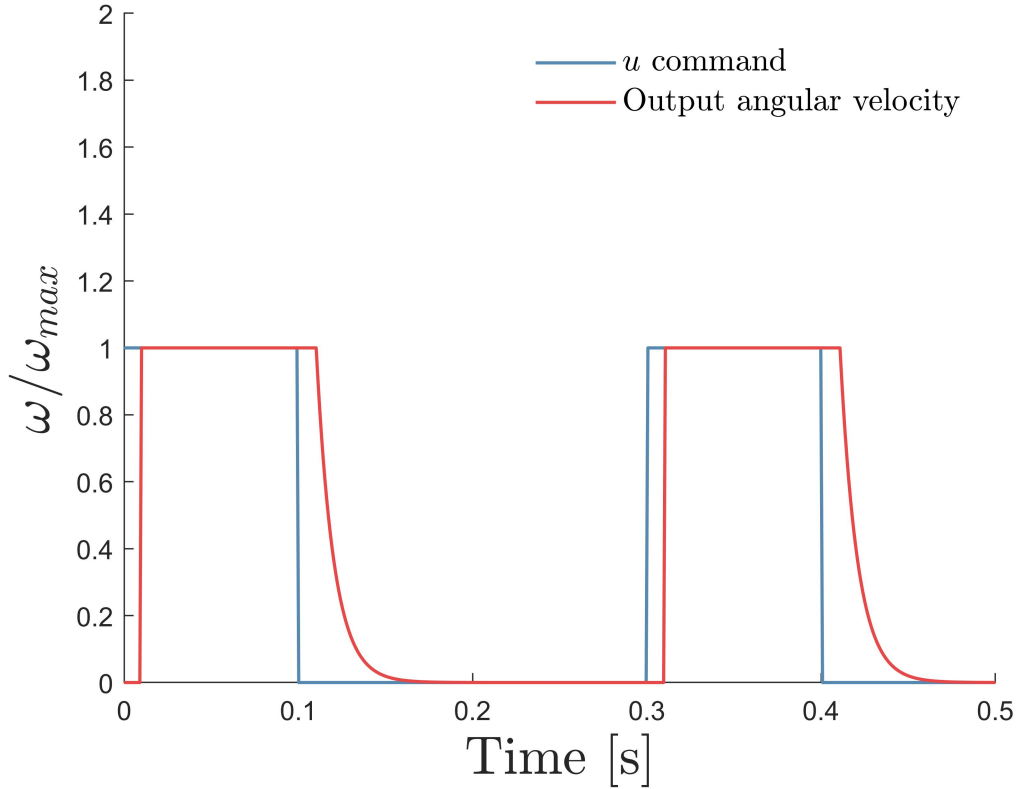


Figure 2.8: Graph shows how engagement delay and friction affects output angular velocity

In order to compensate such delay we followed the approach of Integral Control as described in [20] and fully applied by Xie in [19].

The idea is that the ideal architecture we have described above is memoryless, but delay and friction introduce a time shift thus the error gain needs a memory. An integral block of the error is added to the proportional one to satisfy this issue.

2.4 Low level control architecture: PWM modulated by PID

In this section it is showed the implementation of the control system described. In particular, it is possible to appreciate the PWM generator and the logic command for relays. The reference $r(t)$ for the controlled system is a trajectory θ_d that the pulley has to follow, therefore the loop is closed in position. PID stage modulates the error and it is saturated between $[-1, +1]$ in order to give, as input for the PWM generator, a proper duty ratio.

In Figure 2.9 it is possible to visualise the actual control system.

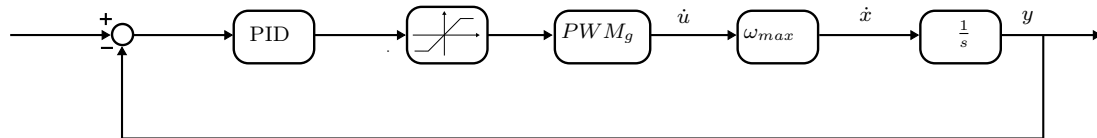


Figure 2.9: Schematics of the PID PWM control system

2.4.1 PWM Generator

PWM Generator has to keep as input a signed duty ratio and it has to provide, as output the command for the clutches. First of all, we need to sample the PID output at a fixed frequency $f_{PWM} = 1/T_{PWM}$. The absolute value of the sampled PID is the duty ratio $\tau_{PWM}(e(t_k))$. The sign is needed in order to choose if the command has to be positive (+1) or negative (-1).

Then, we want that at t_k the state of the PWM generator has to switch from 0 position to 1 and hold this state for a time $\tau_{PWM}[e(t_k)]T_{PWM}$. This result is achieved comparing the value of a decreasing sawtooth with unitary amplitude and period equal to T_{PWM} . In Figure 2.10 is showed the implementation of the actual PWM Generator and in Figure 2.11 it is possible to visualise the comparison between sawtooth signal and duty ratio and, then, the output.

2.4.2 Logic Port

The logic port has to interpret the output of PWM Generator and to transform it in a command for relays in order to activate forward, backward or brake clutch. Here is the pseudocode of the MATLAB implemented logic.

Algorithm 1 Logic port

```
1:  $u \leftarrow$  Output of PWM Generator
2:  $fClutch \leftarrow$  forward clutch
3:  $rClutch \leftarrow$  reverse clutch
4:  $bClutch \leftarrow$  brake clutch
5: if  $u = 0$  then
6:    $bClutch \rightarrow ON$ 
7:    $rClutch \rightarrow OFF$ 
8:    $fClutch \rightarrow OFF$ 
9: else if  $u = 1$  then
10:   $bClutch \rightarrow OFF$ 
11:   $rClutch \rightarrow OFF$ 
12:   $fClutch \rightarrow ON$ 
13: else if  $u = -1$  then
14:   $bClutch \rightarrow OFF$ 
15:   $rClutch \rightarrow ON$ 
16:   $fClutch \rightarrow OFF$ 
17: end if
```

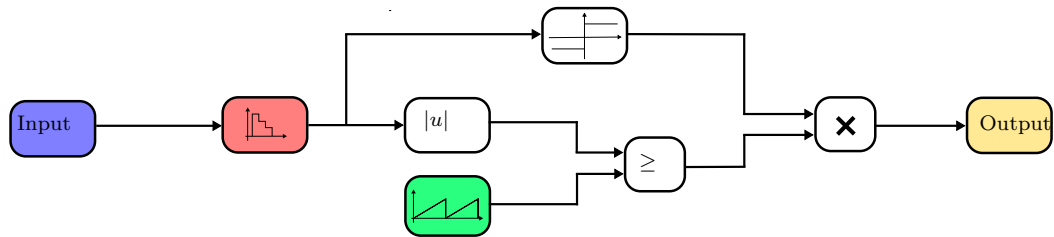
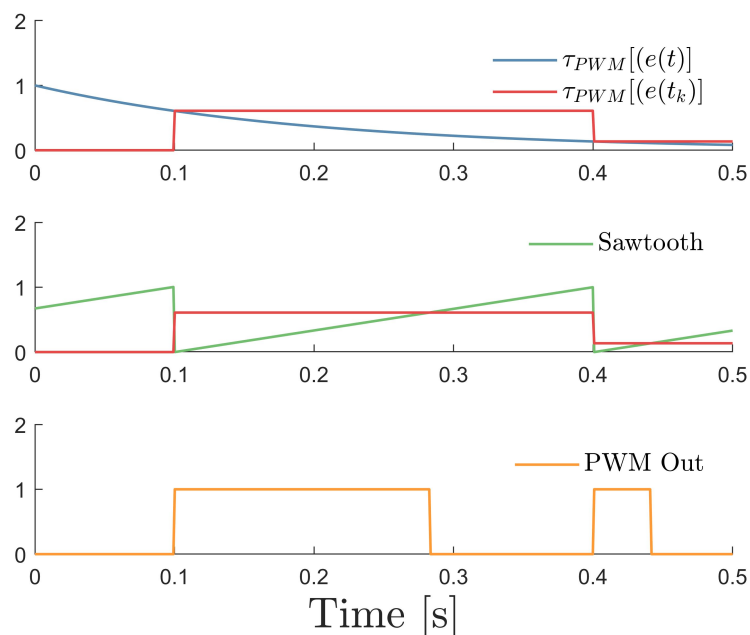


Figure 2.10: Schematics of the PWM Generator


 Figure 2.11: Graphics summarizing the working principle of a PWM Generator, assuming a $T_{PWM} = 0.3s$

2.5 High level control: admittance control

The controller developed in this section has been used to generate trajectories as reference signal for low level controller. The aim of this control strategy is to assist users in elbow flexion/extension movements whilst compensating for the forearm's weight. A full description of the architecture is described in [27]. In this work we adapted that model with our actuator. In fact, in the strategy developed by Chiaradia the DC-motor was controlled closing the loop in velocity. In this case, we used the same algorithm to evaluate a position reference for the module.

The control algorithm has to fulfill two requirements:

1. Providing assistance;
2. Not obstructing natural movements.

The proposed solution provides assistance by compensating gravitational field forces. Thus, it requires the ability to track a position dependent force profile that is equal in magnitude and opposite to gravitational field acting on the forearm. The second objective requires transparency of the suit to the user’s movements, in other words backdrivability. This, theretically, can be achieved mechanically because it is possible to disengage each clutch, but losing assistance. Furthermore, Bowden cables make the transmission inefficient due their own sitiffnes. We need to achieve backdrivability by control.

The proposed controller is shown in 2.12. It comprises an outer torque loop that provides a position reference for the low level control described in 2.4. The former is responsible for tracking the position-dependent torque profile at the elbow. In practice, it computes a motion reference as an interaction torque is sensed, thus creating virtual backdrivability. Differently from the classical admittance implementation, this inner position loop is closed at the motor level instead of at the joint level. This approach, known as collocated admittance control [33], has been shown to robustly deal with force disturbances such as stiction and backlash [35], abundant in the soft exosuit.

2.5.1 PID Admittance control

The torque acting on the elbow joint as a result of gravity is estimated using a simple single-joint model and assuming that the arm is adducted on the side of the trunk:

$$\tau_g = mgl_c \sin \theta$$

with m being the combined mass of the forearm and hand, l_c the distance of the center of gravity of the forearm and hand from the center of rotation of the elbow joint, g the acceleration of gravity and θ the elbow angle, assumed to be zero in the fully-extended configuration.

To estimate the torque at the elbow joint provided by the exosuit we need to introduce an extension function that links displacement of the tendon cable to the angle of the elbow. Referencing to 2.5.1, we can define two extension functions:

$$h_f(\theta) = 2\sqrt{a^2 + b^2} \cos\left(\phi + \frac{\theta}{2}\right) - h_{f0}$$

$$h_e(\theta) = R\theta - h_{e0}$$

If we define $P(\theta)$ to be the matrix mapping the tension in the tendons, f , to the torque on the joints , τ_{exo} , we can derive:

$$P(\theta) = \frac{\partial h^T}{\partial \theta}$$

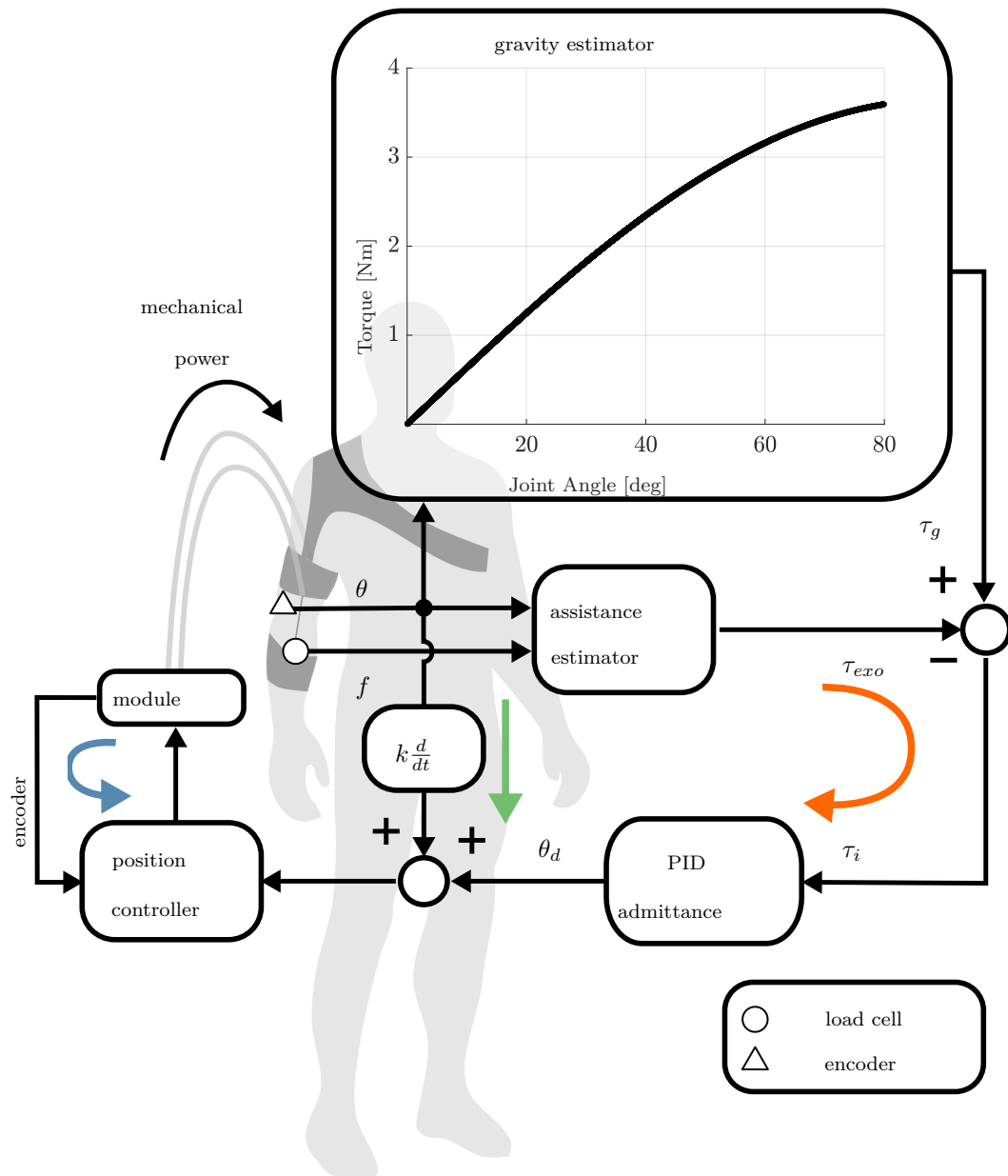


Figure 2.12: An outer torque loop (orange) tracks a reference profile equal and opposite to gravity, computing a motion reference as an interaction torque is sensed, according to the admittance specified by a PID controller. The low level control (light blue) is closed on the module position. The green arrow indicates a positive feedback path, introduced to improve transparency.

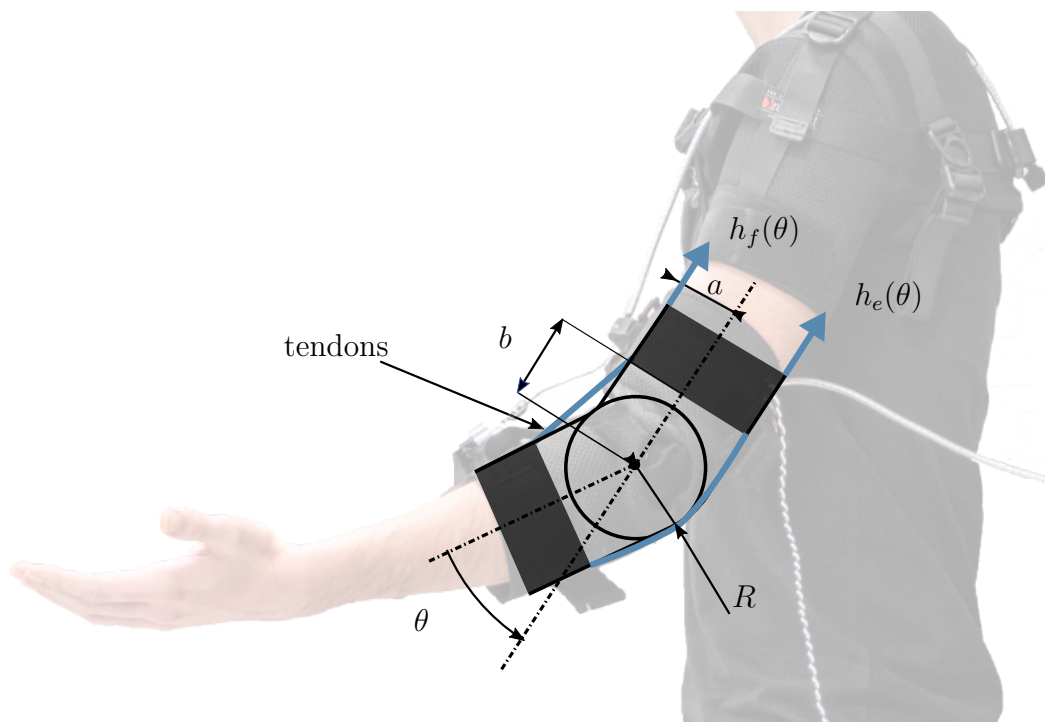


Figure 2.13: Routing of the tendons along the elbow exosuit

The assistive torque is estimated by multiplying the tension measured by the load cell, f , by its moment arm $P(\theta)$:

$$\tau_{exo} = P(\theta)f$$

The difference between τ_g and τ_{exo} , i.e. the interaction force, τ_i , between the suit and its wearer, is converted to a reference position θ_d for the motor by a specified admittance. Being one of our requirements that of transparency, τ_i must be set to zero. The admittance can assume the form of a PID controller [31]:

$$Y(s) = \frac{\theta_d}{\tau_i} = Ps + I + \frac{D}{s}$$

with the P, I and D constants governing the characteristics of the relation between the interaction force and the exosuit's kinematics. The PID parameters were initially set using the tuning rules described in [31] from the human elbow impedance parameters identified in [32]. A heuristic fine-tuning for each subject was performed in a familiarisation phase prior testing the device. An additional positive feedback term, proportional to the speed of the elbow joint, increases the sensitivity of the device to its wearer's movements. As elegantly discussed in [33], this comes at the expense of a loss in robustness, so extra care needs to be taken when tuning the outer admittance loop.

2.6 Electro-mechanical hardware

2.6.1 DC motor

The driving motor that excites the module to reach its maximum angular velocity ω_{max} is a MAXON EC-i 40 70W. A second motor, of the same kind and characteristics has been used to impose a load during loading behavior test.

2.6.2 Clutches

Electromechanical clutches from Inertia Dynamics, SO series, are typically used to connect two inline shafts. In this case, the armature hub assembly is connected to the load shaft as usual, but the rotor assembly is externally connected to a frame that links the armature to the corresponding gear. The brake clutch works connecting the armature hub to a clamped shaft. In Figure 2.15 you can see a picture of the adopted clutch.

2.7 Electronic control hardware

In this section it is described electronic hardware that implements control algorithm, runs it, collects sensors' signals and drive the actuator.

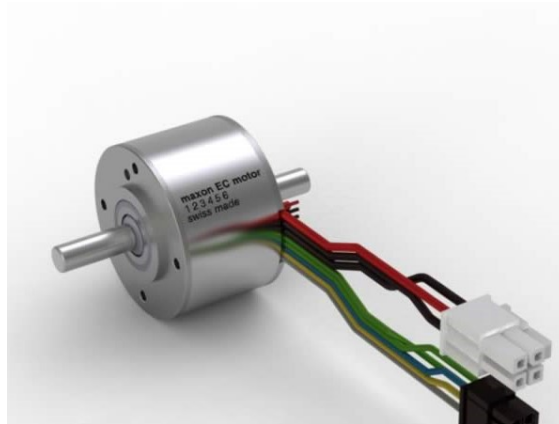


Figure 2.14: Picture of the DC motor



Figure 2.15: Picture of the electromechanical clutch from catalogue

2.7.1 Test bench

Test bench is composed by a Data Acquisition device and driver for motors.

Quanser QPIDE

Quanser QPIDE¹ is a control device that via an internal software automatically generate a code from Simulink model. This code runs the control algorithm, using data collected from peripherals and imposing control's commands to relays and motor

¹<https://www.quanser.com/products/qpide-data-acquisition-device/>

drive. It runs the software at a sampling frequency $T_S = 1$ KHz. In Figure 2.16 there is a picture of the Quanser board.



Figure 2.16: Picture of the Quanser QPIDE

EPOS 50/5 Motor Drive

The selected motor driver is the EPOS2 50/5², which is a modular, digital positioning controller by maxon motor. It is able to perform lowlevel EC motor control with a desktop application easily. Most of the testing has been done with Velocity Control, so that the Motor shaft runs with a constant speed. The motor driver is used to:

- provide a power supply to encoder;
- control the motor;
- communicate with the supervisory controller (Quanser).

The unit has been operated via USB. EPOS works as slave driver, receiving commands from Quanser. In Figure 2.17 there is a layout of connections of the motor drive.

²https://www.maxonmotor.com/medias/sys_master/root/8827037122590/17-EN-431-432-433-435.pdf

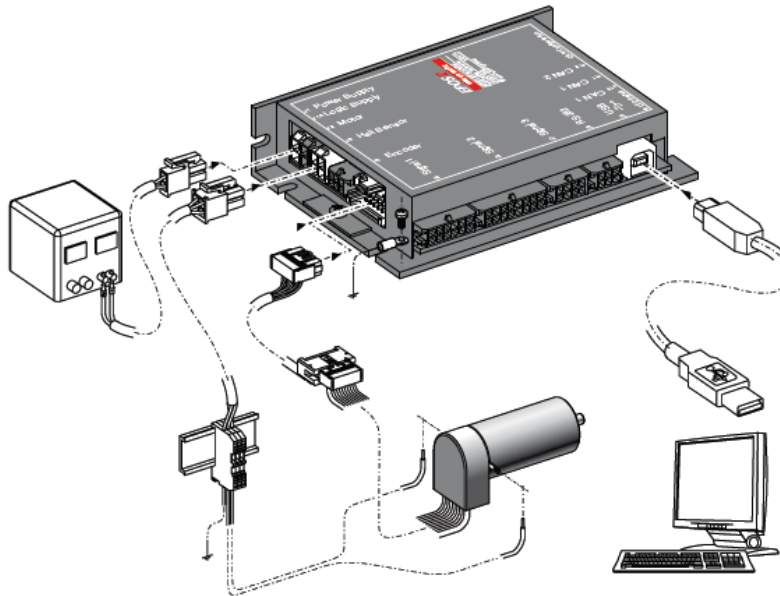


Figure 2.17: Connections layout of EPOS2 50/5 from catalogue

2.7.2 Relays

We used an Opto-Isolated Relay Module - 4 channels [2.18](#). Relays have to engage or disengage clutches, closing or opening their power supply circuit. The circuit of each channel of the relay can work in two operating conditions: normally open (NO) or normally closed (NC). Thus, in this case, circuit is normally open and the correspondent clutch is disengaged. The control signal is a voltage: $0V$ implies to keep the state in NO, $5V$ closes the circuit. In [Figure 2.19](#) you find a schematic of the circuit of the relay.

2.8 Sensors

The prototype uses a set of sensors to implement the control architecture and to evaluate performances. In detail:

1. The low level control closes its loop in position and uses an encoder on the main shaft of the module;
2. The admittance control uses an encoder on the elbow and a cell load at the end of the of the flexor cable;
3. To evaluate the reduction of neuromuscular activity we used EMG during a trial on the biceps brachii muscle, positioning of the sensor followed the SENIAM standard.

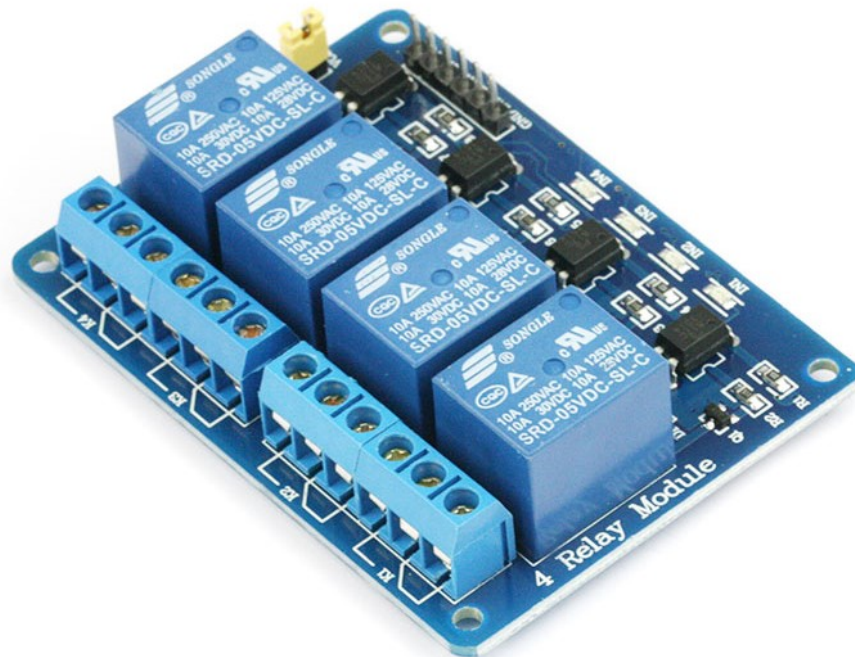


Figure 2.18: Picture of the relay module

In the next paragraphs there are descriptions of these sensors and methods implemented to correctly interpret their signals.

2.8.1 Shaft Encoder

On the main shaft we put an incremental encoder, connected through an Oldham coupling. Its output cable is connected directly to an analog input port of the Quanser. Its resolution is $200P/R$. Thus the output firstly has to be converted in *rad* and, to have a good signal as feedback filtered. We used a second order Butterworth filter with a cutoff frequency of $25Hz$. The encoder is an OMRON E6A2-CWZ3E 200P/R 0.5M³. In Figure 2.20 there is a drawing of the encoder.

2.8.2 Load Cell

The output has been calibrated:

- In no load condition offset is evaluated and then compensated

³<https://www.ia.omron.com/product/item/2373/>

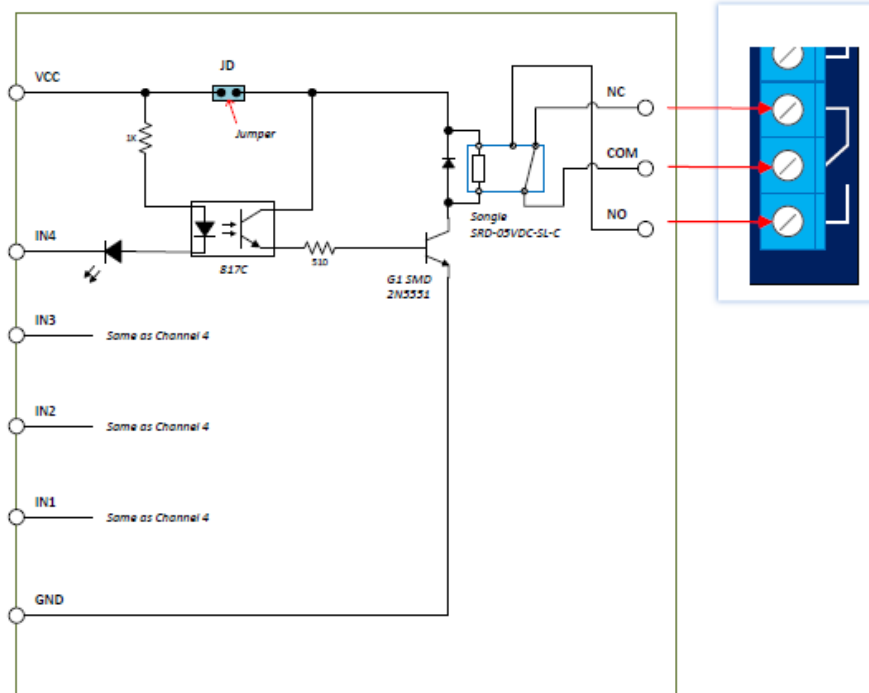


Figure 2.19: Schematic of a single Module of the Relay

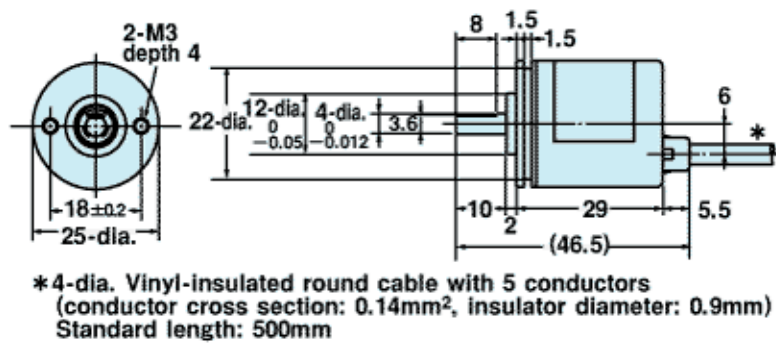


Figure 2.20: A picture of the load cell

- Using known mass items we adjusted the gain.

In this way we obtained a linear characteristic of the sensor⁴. In Figure 2.20.

⁴<http://www.futek.com/index.aspx>

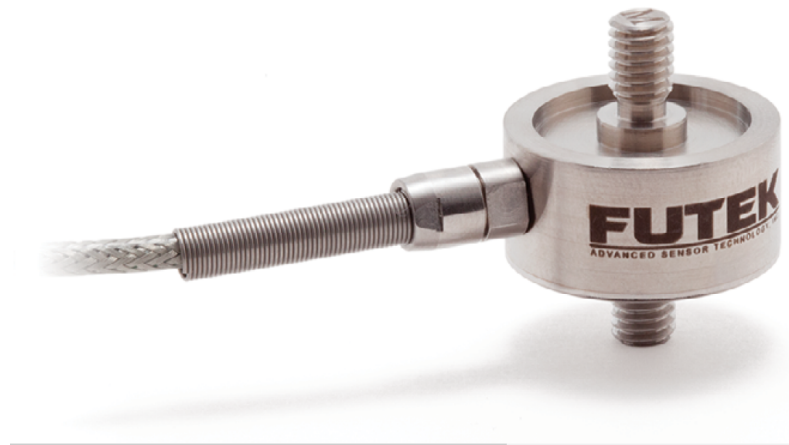


Figure 2.21: Drawing of the encoder from catalogue

2.8.3 Elbow Encoder

It is an absolute encoder (AMS, AS5047P, 1000 pulses/rev). It is mounted to a double flanges frame. One end is connected to the arm and the other one to the forearm: in this way the encoder measures the elbow angle.

2.8.4 Surface EMG

Muscular effort is estimated from the Root Mean Square (RMS) of the Electromyography (EMG) of the main muscle involved in performing elbow flexion movements, i.e. the biceps brachii. We positioned the electrodes according to the SENIAM standards [26]. The raw EMG was acquired using an external sensor, i.e. Trigno wireless EMG sensors (Delsys Inc.). It was acquired by the Quanser, then pre-processed in Matlab Simulink using a full-wave rectification and low-pass filtered by a second-order Butterworth filter with a 8Hz cut-off frequency. This signal is normalized according the MVC: Maximum Voluntary Contraction.

Chapter 3

Characterization and Performances Evaluation

In this chapter we show a documentatation of the main results of this design. In particular, in the first section there is the documentation on how we chose parameters of the low level control: T_{PWM} and PID. The second and third sections contain the descriprion of the experiments to characterise the system: bandwidth and behavior in loaded conditions. The last section is focused on performances of the exosuit when it is used by an healthy subject.

3.1 Tuning Parameters

As we have seen in section 2.3 we need to choose and set parameters for the control system. In the next paragraphs it is explained how we chose the frequency of the PWM Generator and parameters of the PID block.

3.1.1 T_{PWM}

T_{PWM} is the most crucial parameter of the control system in fact the main assumption that garantees stability is that the frequency of sampling process has to be great enough in order to confuse a sampled instant t_k with the continous time t . There are two constraints that limit a lower bound for T_{PWM} :

1. T_S , the sampling time of the system during which software is ran to compute states and outputs;
2. δ , the time delay due to engagement and disengagement of clutches.

It is evident that $\delta \gg T_S$ and, in fact, in 2.7 it is showed in detail characteristics of the the hardware. Therefore, as stated in the Nyquist-Shannon Theorem [25], the

T_{PWM} is lower bounded by 2δ . This constraint is not enough. We have already explained that the disengagement phenomenon is affected by a viscous friction. It is not the aim of this work to build a proper model of this phenomenon and then identify its internal parameters. Karbasi [23] proposed an approach of this kind. In this case, we performed some tests on the actuator to justify the choice of T_{PWM} . Setting the prime velocity ω_{max} to a constant value and then controlling the the motor in velocity, we performed an experiment imposing increasing value of the signed duty ratio to the PWM Generator. In figure 3.1 it is showed the beahavior of the system using different T_{PWM} . This graph allows to visualise the effect of the delay on the ability of the actuator to modulate different fractions of the ω_{max} . Considering that we want to obtain an almost linear relationship between duty ratio and normalize angular velocity, it is possible to evaluate the linearity of each plotted curve through the coefficient of determination R^2 factor. In table 3.1 you can see different values of this factor. Therefore we choice of T_{PWM} is a trade off between the specification of linearity and the need of having a PWM frequency as high as possible. We set this parameter to $T_{PWM} = 0.3s$.

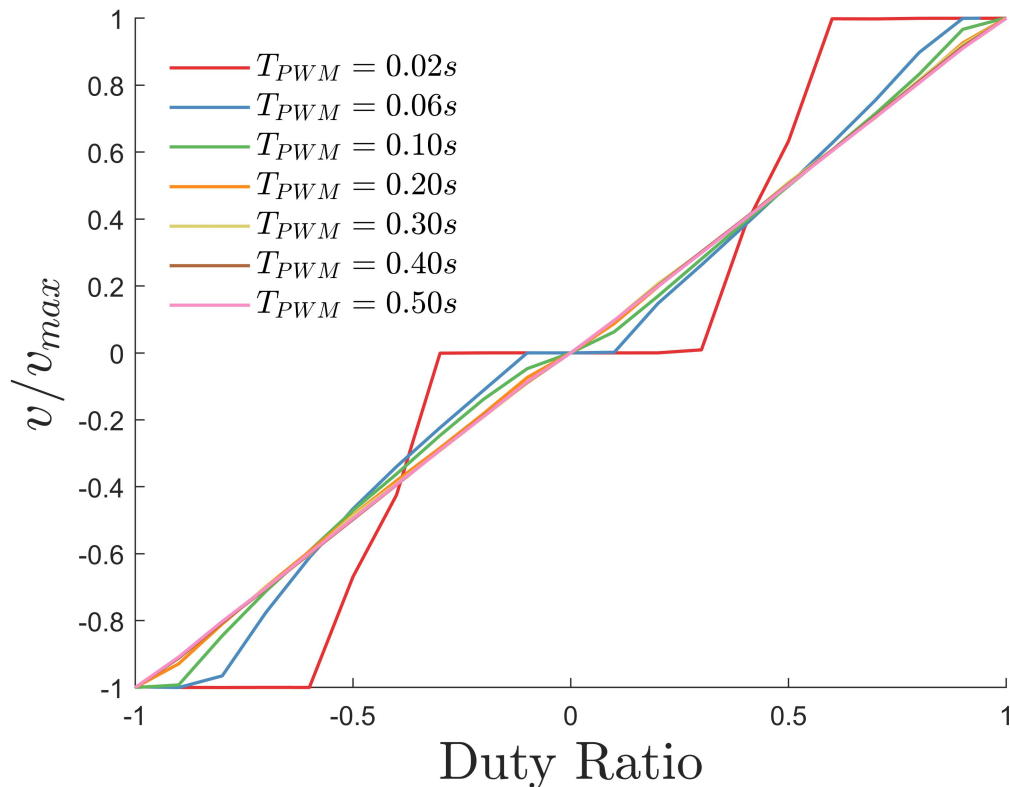


Figure 3.1: Duty Ratio effect at different T_{PWM}

$T_{PWM}[s]$	R^2
0.02	0.93655
0.06	0.98944
0.10	0.99654
0.20	0.99602
0.30	0.99876
0.40	0.99917
0.50	0.99929

Table 3.1: R^2 evaluated for curves of Figure 3.1

3.1.2 Tuning PID

In order to tune PID parameters we have taken into account performance specifications to be fulfilled:

1. Minimizing overshoot in response when the input is a step;
2. Minimizing the error when the input is a ramp.

PID parameters are subjected to the influence of ω_{max} . In fact, it is simple to see that if the maximum velocity that the module can fulfill is higher than the proportional factor, for example, has to be lower. Thus, for each choice of ω_{max} it is needed to re-tune the controller. From this point of view there is no interest in seeing what is the response of the system to the step. The reference that is relevant is the ramp. In fact, it is possible to study what is the behavior of the system when the reference is a ramp with slopes that are fraction of the maximum angular velocity. The expected result is that the higher is the velocity, the lower will be the error.

In figure 3.2 you can find the experimental setup that we used to evaluate the influence of the slope desired on the tracking error. Figure 3.3 shows a sample of different experiments we performed. In particular, you can see that when ω_{max} is high enough we have a negative error, $e = r(t) - y(t)$ and the system, in certain instants, is behaving in advance of the input.

We performed this experiment for different values of ω_{max} , imposing equally spaced desired slopes in $[-\omega_{max}, \omega_{max}]$. In figure 3.4, you can see the value of RMSE for each desired angular velocity. As expected error grows with the desired velocity. Furthermore, error decreases with the ω_{max} . But, the effect of forward behavior above described results in a higher error when the desired velocity is near to $|\omega_{max}|$. In section 3.2, we will see how this phenomenon affects bandwidth of the system.

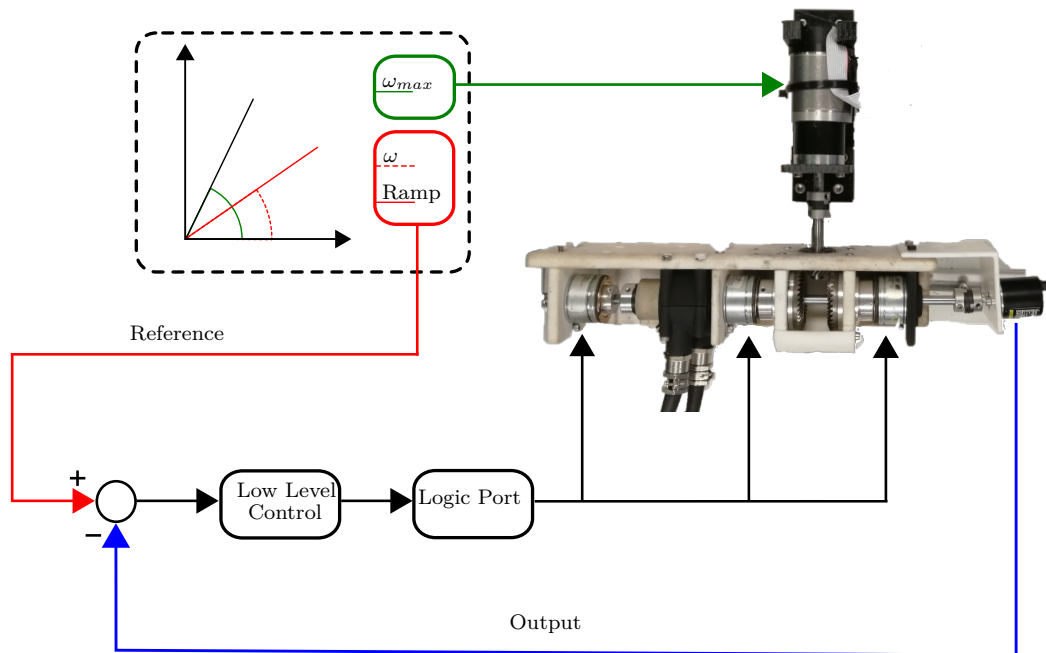


Figure 3.2: Experimental setup for evaluating ramp trajectory tracking. The reference is a ramp with slope ω that is a fraction of ω_{max} . Low level control produces an input u for the logic port that sends commands to clutches.

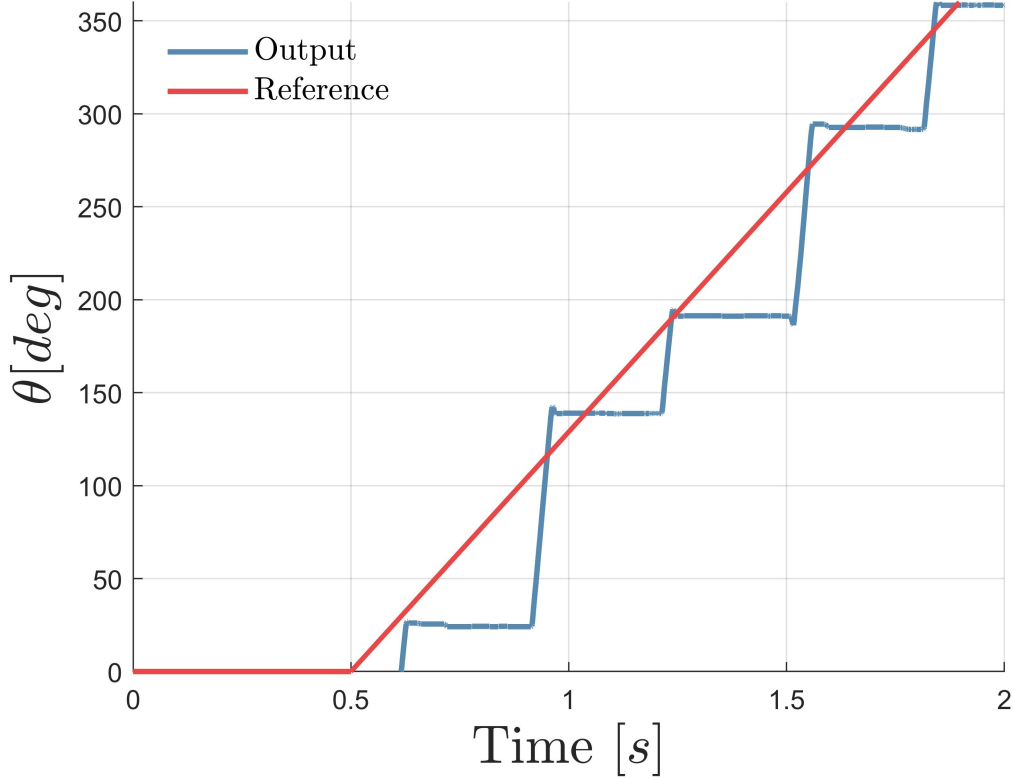


Figure 3.3: A sample of I/O response of the system when the reference is a ramp. In this case $\omega_{max} = 45rad/s$

3.2 Bandwidth

In order to characterize the module in frequency domain we performed the same experiment described in [24]. In this case we imposed different values of ω_{max} . Each test is performed collecting for each maximum velocity a set of sine wave responses equally spaced in frequency domain covering $f \in [10^{-2}, 1.1]$ ($[f] = Hz$). The sine wave reference is:

$$r(t) = A \sin(2\pi ft)$$

Where A is the correspondent amplitude of $90deg$ of elbow joint. In Figure 3.5 it is shown the setup of this experiment and in Figure 3.6 a sample of the output response when the input is a sine wave. In particular, you can see that, in general, the system follows the input reducing its amplitude. For each couple of sine wave it is possible, by Fourier transform of the output, to evaluate the complex ratio between output and input. Without taking into account higher order components of Fourier transform but just the first, this ratio in amplitude and phase represents

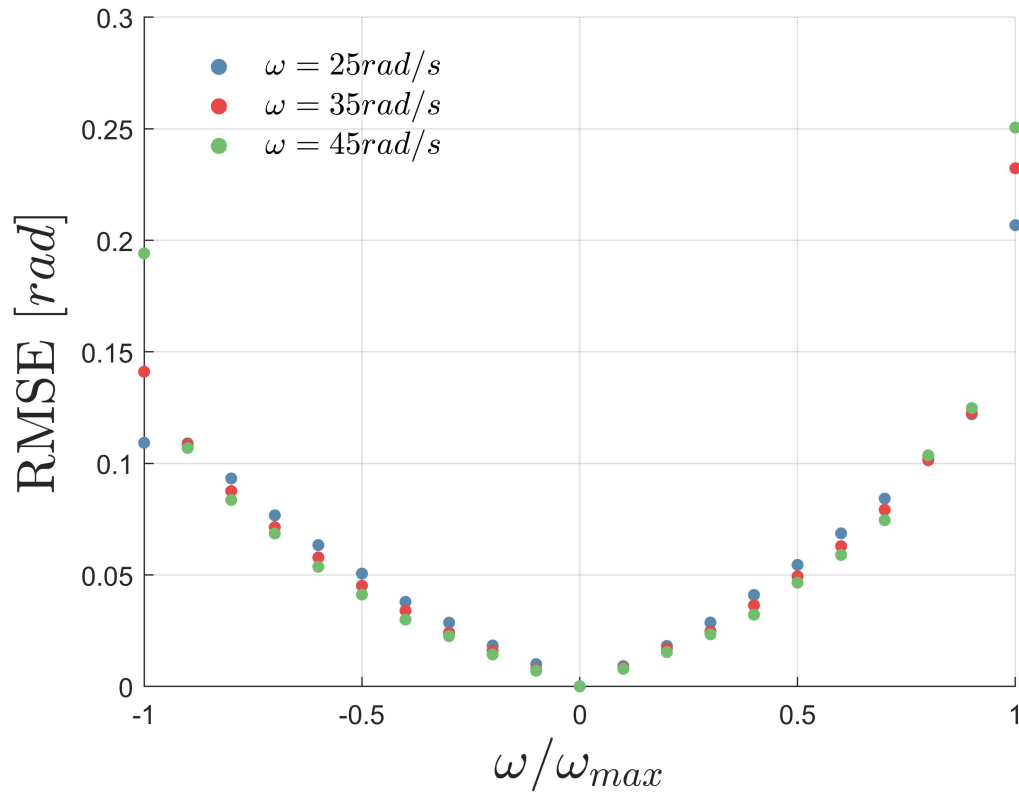


Figure 3.4: The influence of ω_{max} on tracking performance of the actuator: evaluated by $RMSE$ of the output position and ramp references with slopes fractions of the maximum velocity

a point in the Bode Diagram. In Figure 3.7 are shown results of this test performed with different maximum velocities. From this graph it is possible to evaluate the cutoff frequency f_c of the system: when the amplitude is reduced by $-3dB$ (Table 3.2).

As Canesi showed in [24] it is possible to see that the cutoff frequency increases

$\omega_{max}[\text{rad/s}]$	$f_c[\text{Hz}]$
25	0.88
35	1.26
45	1.51
55	1.30

Table 3.2: Cutoff frequencies for different values of ω_{max}

whit ω_{max} . It is worth to compare results of this experiment with those performed

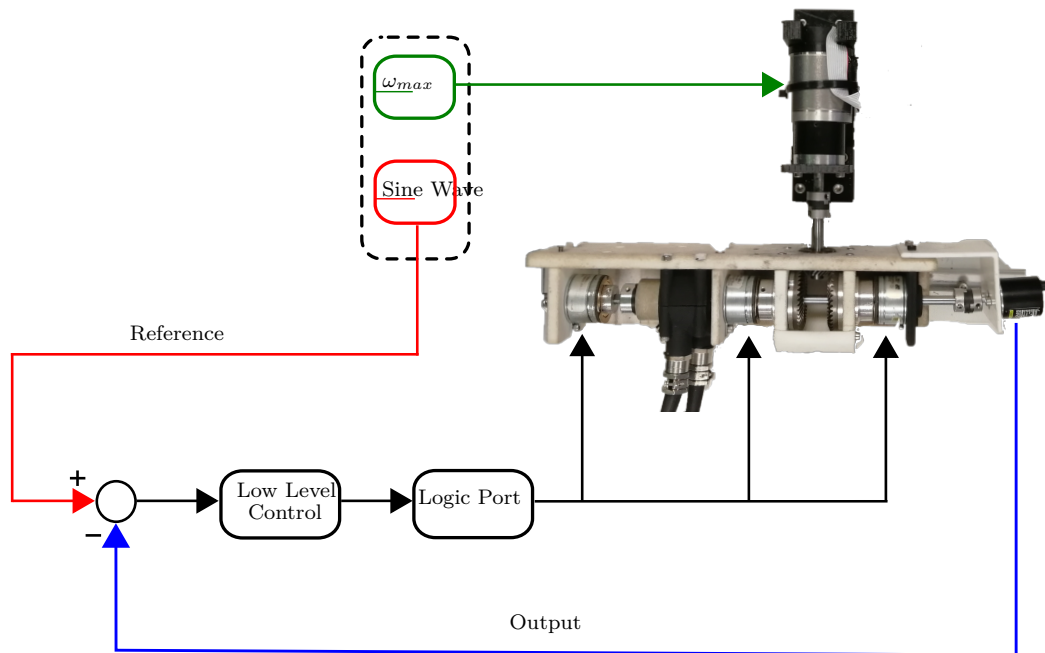


Figure 3.5: Experimental setup for evaluating ramp trajectory tracking. The reference is a ramp with slope ω that is a fraction of ω_{max} . Low level control produces an input u for the logic port that sends commands to clutches.

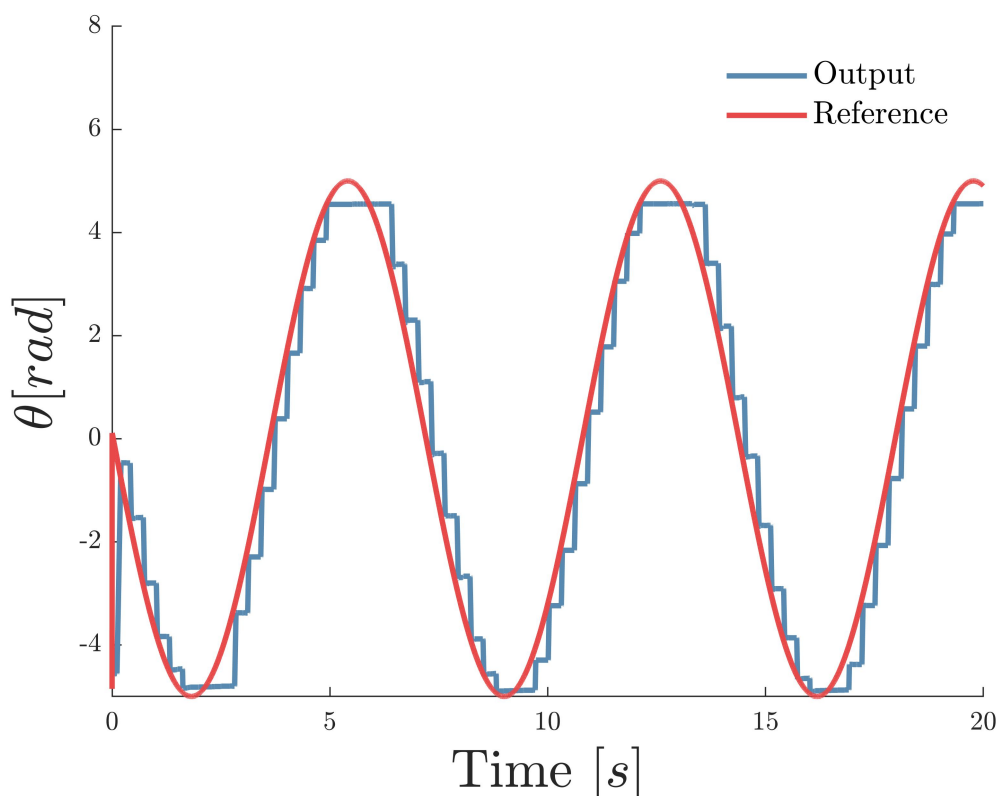
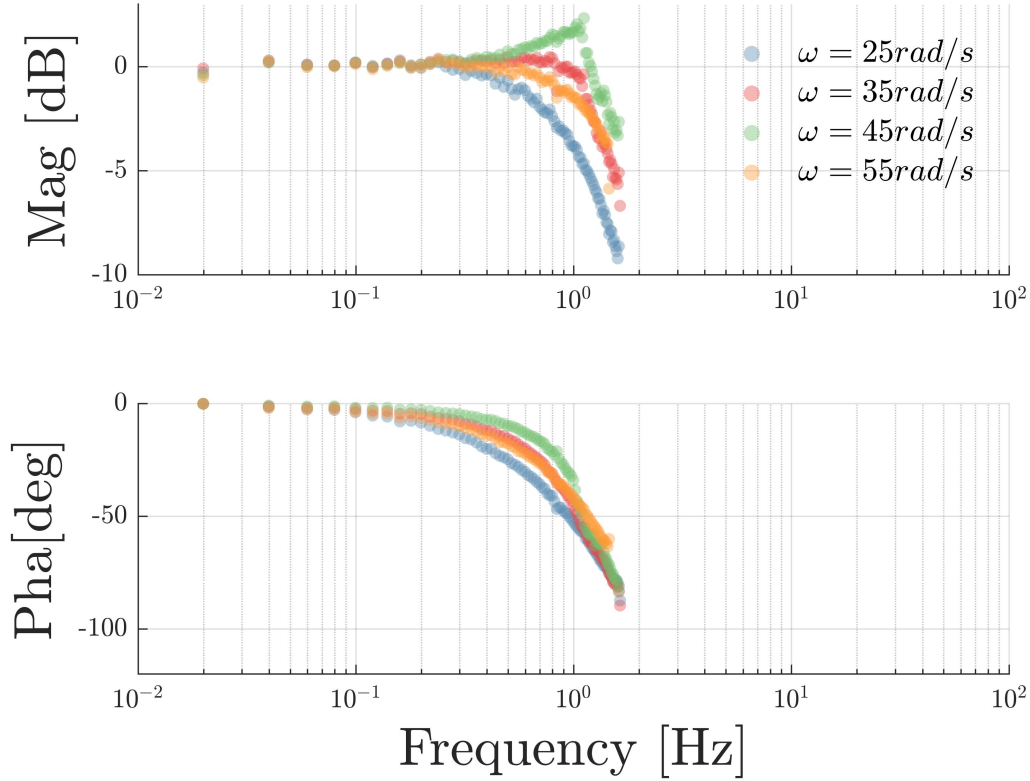


Figure 3.6: A sample of I/O response when the reference is a sine wave

by Canesi.

The first difference is that the cutoff frequency is almost similar to the previous module but slightly lower. The reason is that the control algorithm implemented here works in late respect to the state machine earlier developed. The state machine, behaves maintaining a limited error in module without taking into account the sign. This results in an higher bandwidth but also in a non negligible time in which the system works in advance of the reference.

Another difference is that for $\omega_{max} = 45rad/s$ we observe the presence of a resonance peak. This is the effect that we underlined in the previous section. In fact, when the system is excited by that ω_{max} the normalized angular velocity requested at certain frequencies is near to 1, with an increasing of positive error. On the other hand, for higher values of ω_{max} this effect disappears because before starting to ask that range of velocities the time delay of clutches starts to saturate the bandwidth. It is, however, worth to perform more experiments to investigate the nature of resonance and validate this hypothesis.

Figure 3.7: Bode diagrams at different values of ω_{max}

3.3 Loaded Behavior

Finally, to characterize the system we performed a test to evaluate its behavior under a load. The setup is shown in Figure 3.8. We assumed as reference a sine wave trajectory with a frequency $f = 0.2 \text{ Hz}$ such that the error is not affected by bandwidth. The amplitude of the sine wave is correspondent to 90 deg motion of elbow joint. To impose a tension on cables we connected them to a couple of pulleys fixed on the same shaft. The shaft is coupled with a DC motor (Maxon EC-i 40, 70 W), driven in current in order to have constant torque output. The experiment consists in a sweep of different loads equally spaced from 0 N to 11 N . For each load cycle it is computed RMSE in position. The experiment was repeated 5 times. In Figure ?? are represented results of this analysis.

In order to establish a maximum admissible error and, thus, characterize a maximum load for the actuator it is possible to compare this results with the ramp following test in 3.1.2 and, in particular in Figure 3.4. Let assume that the maximum allowable error in loaded conditions has to be lower bounded by those curves. Therefore we can say that the maximum cable's tension has to be lower than 8.2 N .

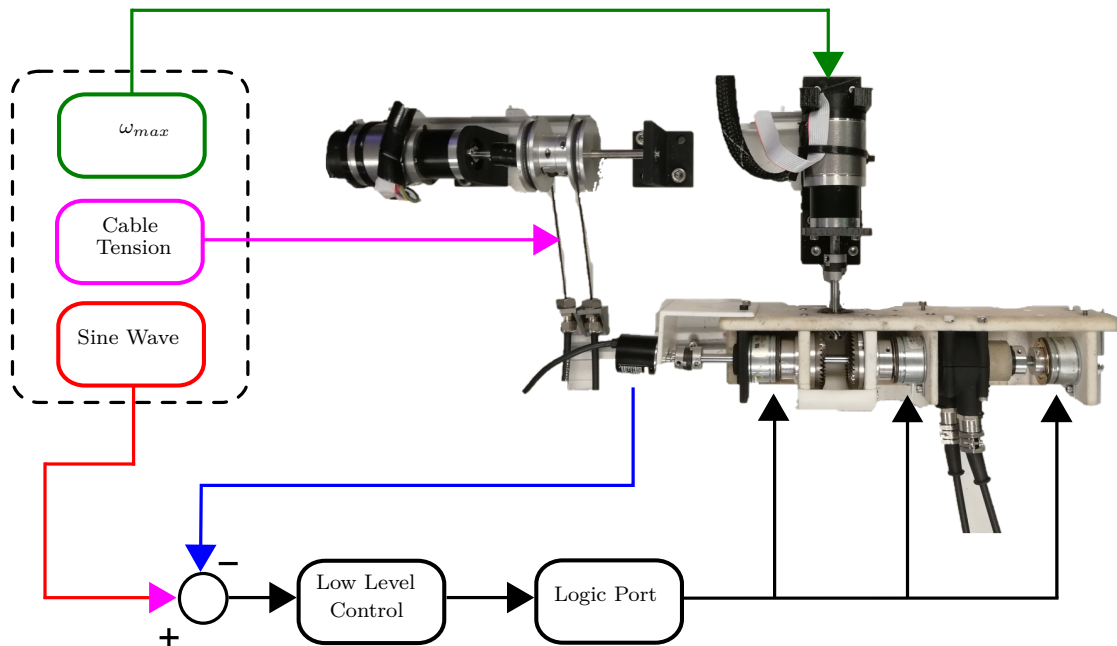


Figure 3.8: Experimental setup for evaluating loaded behavior of the module. The reference is a sine wave with amplitude correspondent to $90deg$. Load is imposed in the sense of cables' tension through driving the second motor in current.

3.4 Test on subject

The aim of the evaluation procedure was to assess the effect of the exosuit on the kinematics and biomechanics of human motion. To do so, we compared biological torque and muscular activation patterns with and without assistance from the device. The testing was done on 1 subject presenting no evidence or known history of skeletal or neurological diseases, and exhibiting intact joint range of motion and muscle strength. The experimental setup is shown in Figure 3.10. The subject had to follow a reference movement performed by a dummy character on a screen, the position of their own elbow being displayed as a superimposed translucent replica of the reference one to provide visual feedback. This was done in two conditions: with and without assistance from the device.

In the latter case the exosuit's tendons were unhooked from the distal anchor point and the motor's power source was turned off. The reference motion consisted of series of Minimum Jerk Trajectories (MJT), known to correspond well to the movements of healthy subjects [40], chosen to be the average elbow speed in activities of daily living (ADLs), i.e. $126deg/s$ [34].

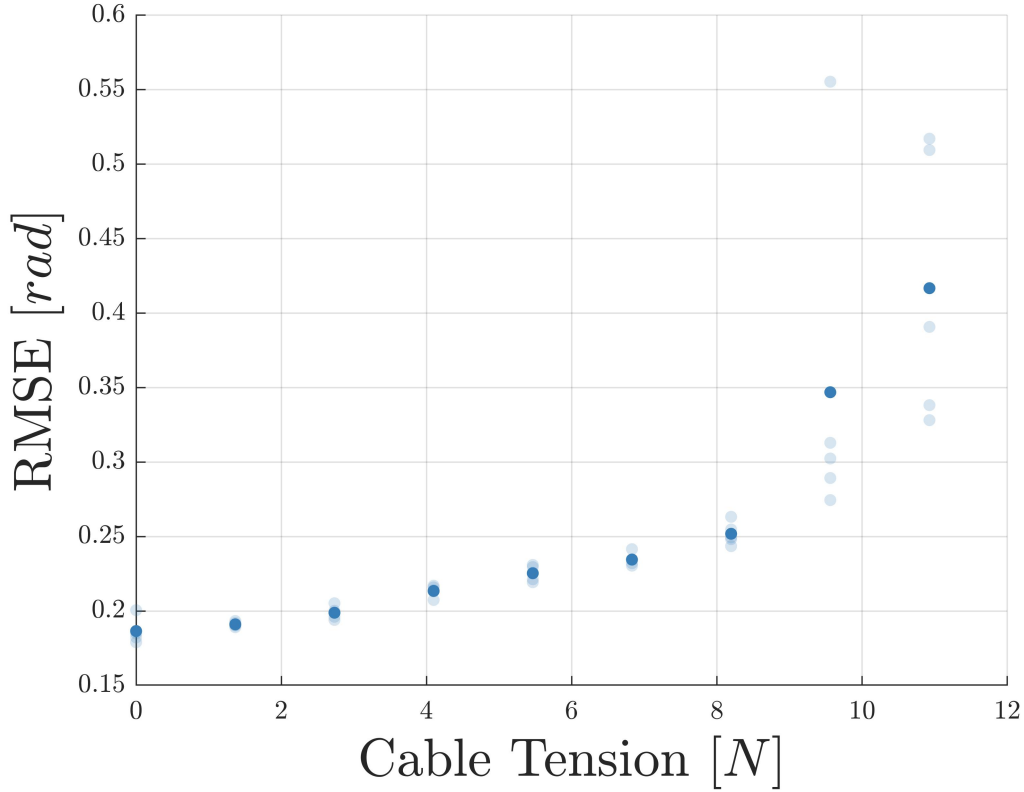


Figure 3.9: *RMSE* of the output position when the reference is a sine wave at constant frequency and cables are in tension with different loads

In order to assess results from EMG analysis and trajectories we performed the same experiment using another actuator described in [27], called from here onwards DC module. In this way, comparing the two datasets it is possible to validate more effectively performances of the prototype.

In Figure 3.11 output trajectories are compared through three conditions: without any assistance, with the OTM module activated, with the DC actuator activated. We can observe that the OTM module behaves fairly well along each cycle, with the exception of the end phase. In fact, trying to stop the arm around the $0deg$ position results to be difficult with a non negligible overshoot. The main reason of this behavior is the late response of the OTM module and you can observe this phenomenon much better analysing torque exchange along each cycle 3.4.2.

3.4.1 Muscular activity reduction

The output EMG signal of the Delsys Trigno system (pre-conditioned with a band-pass Butterworth filter between $20Hz$ and $450Hz$) was processed to extract its

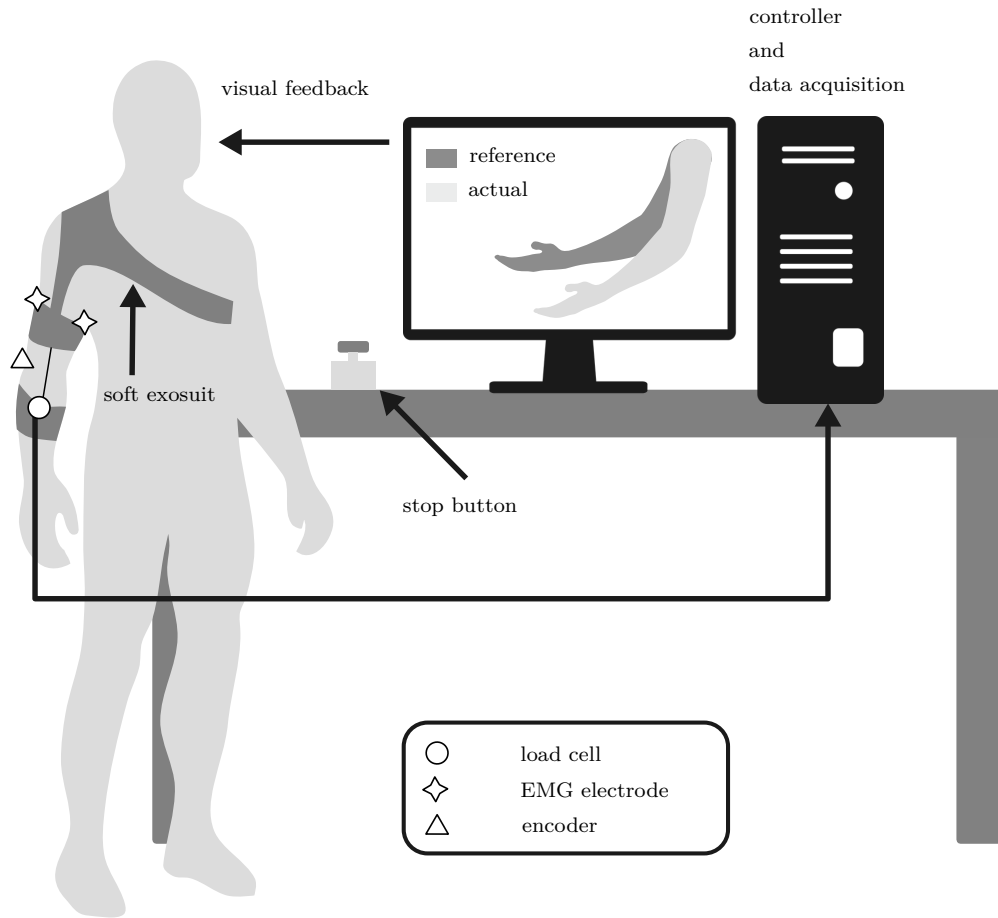


Figure 3.10: Experimental setup for tests on subject

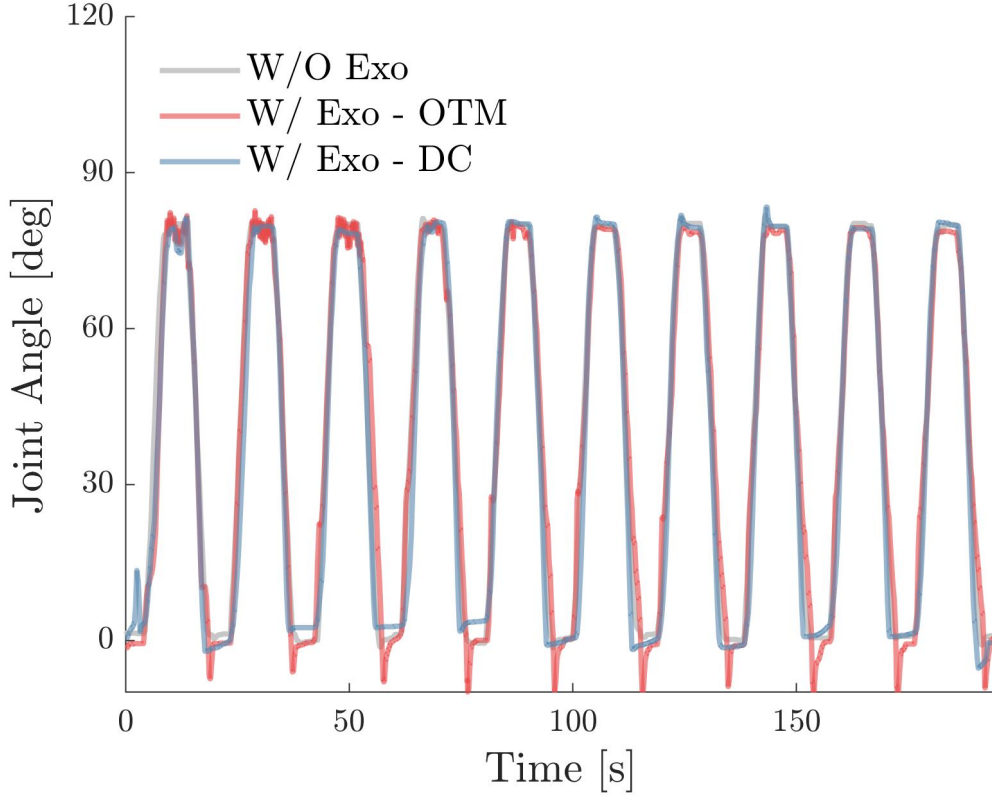


Figure 3.11: Experimental trajectories datasets collected from the elbow encoder in three conditions: in red data acquired using the OTM module, in blue using the DC motor prototype, in grey without any assistance

linear average envelope using the procedure suggested in [35]. This included a whitening operation, to remove correlation between successive samples, a demodulation and relinearization phase, for rectification, smoothing using a moving-average filter (0.2s window) and normalisation by the MVC.

In Figure 3.12 and 3.13 are shown respectively EMG raw signals and EMG envelopes of the biceps during the experiment: without assistance, with the assistance of OTM prototype and the DC one.

It evident that the OTM module needs a period of training before it starts to be assistive. This is not the case of the DC module because the subject was well-trained and confident using that prototype. Then, after familiarisation the OTM shows its effectiveness.

We used the last cycles to measure the level of assistance from electro-myographical point of view. In Figure 3.14 it is showed the overall muscular activity reduction. Despite the fact the change with the module here describe is just 30% compared with 55% of the DC module, it is a good result for a first prototype.

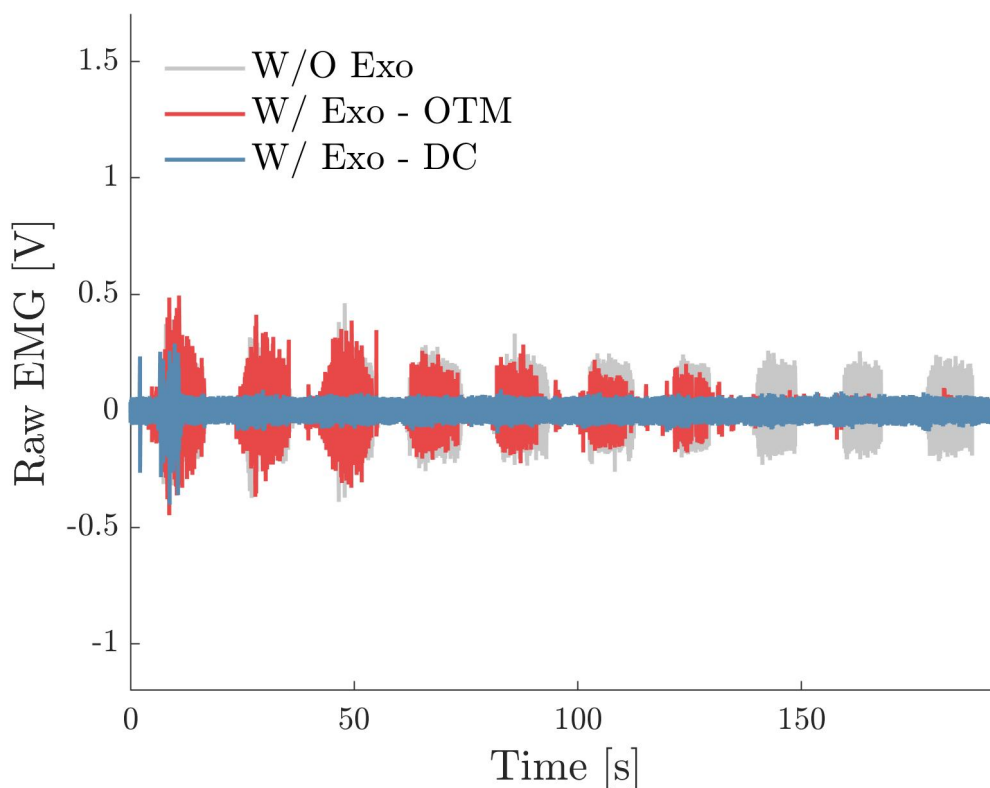


Figure 3.12: Raw EMG signal as acquired. In red the signal acquired using the OTM module, in blue using the DC motor prototype, in grey without any assistance

3.4.2 Torque at the elbow joint analysis

The measured force on the flexing tendon was mapped to a torque on the joint using, as mentioned in 2.5.1, equation

$$\tau_{exo} = P(\theta)f$$

that was used as an estimate of the assistive moment delivered by the exosuit, τ_{exo} . The total torque required to perform the movement was derived from the inverse dynamics of the human elbow, represented as a simple pendulum using a second order model of the form:

$$I\ddot{q} + B\dot{q} + \tau_g = \tau$$

with I being the moment of inertia of the forearm and hand, B takes into account the viscosity of the elbow joint (we used a value of $0.2Nms/rad$ according to the values reported in [32]) and τ_g is the gravity-dependent torque. The difference between the total and assistive torque, $\tau - \tau_{exo}$, was used to estimate the remaining

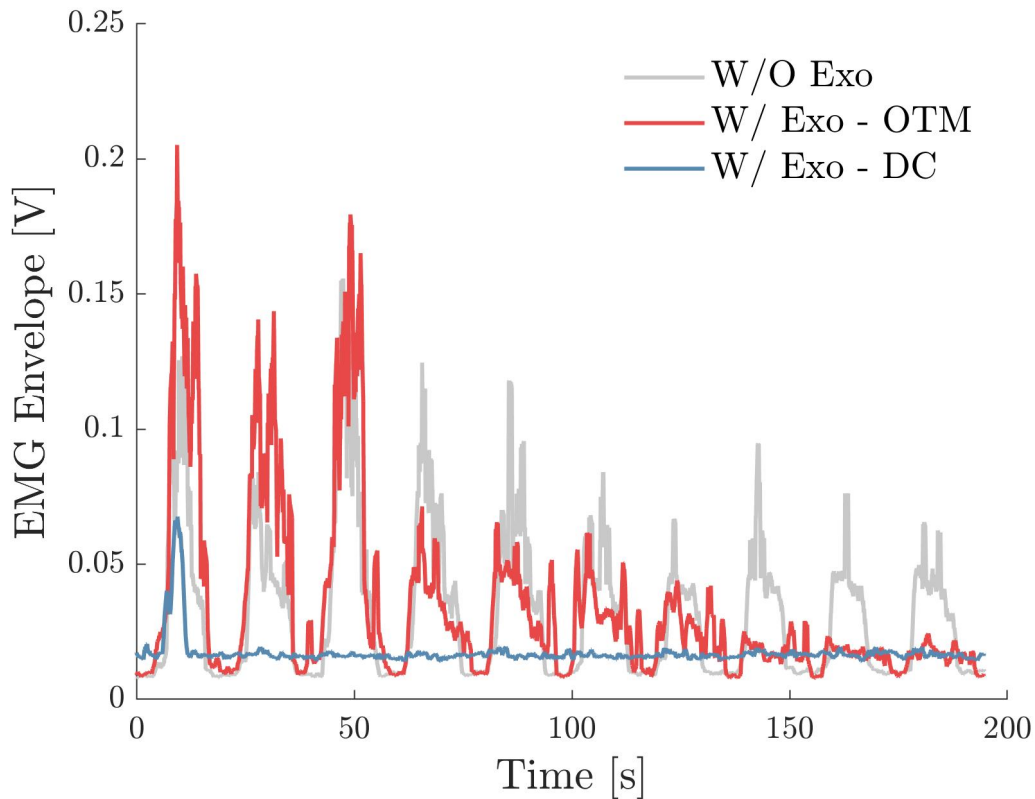


Figure 3.13: The envelope of the filtered absolute value of the EMG signal. In red the signal acquired using the OTM module, in blue using the DC motor prototype, in grey without any assistance

biological torque exerted by the subject to perform the movement or hold the position. In Figure 3.15 it is showed the torque distribution along one cycle between the subject (biological torque) and the exosuit. It worths to see that human torque is not always decreased in module: the effect of late response of the exosuit results in a needing of opposing torque against the exosuit's effort.

In Figure 3.16 this effect is underlined comparing torques in absolute value. It is evident that human subject has to impose an additional force to compensate exosuit when the torque needed is lower than torque produced by the exosuit.

However the overall torque that the subject has to produce is decreased as showed in Figure 3.17.

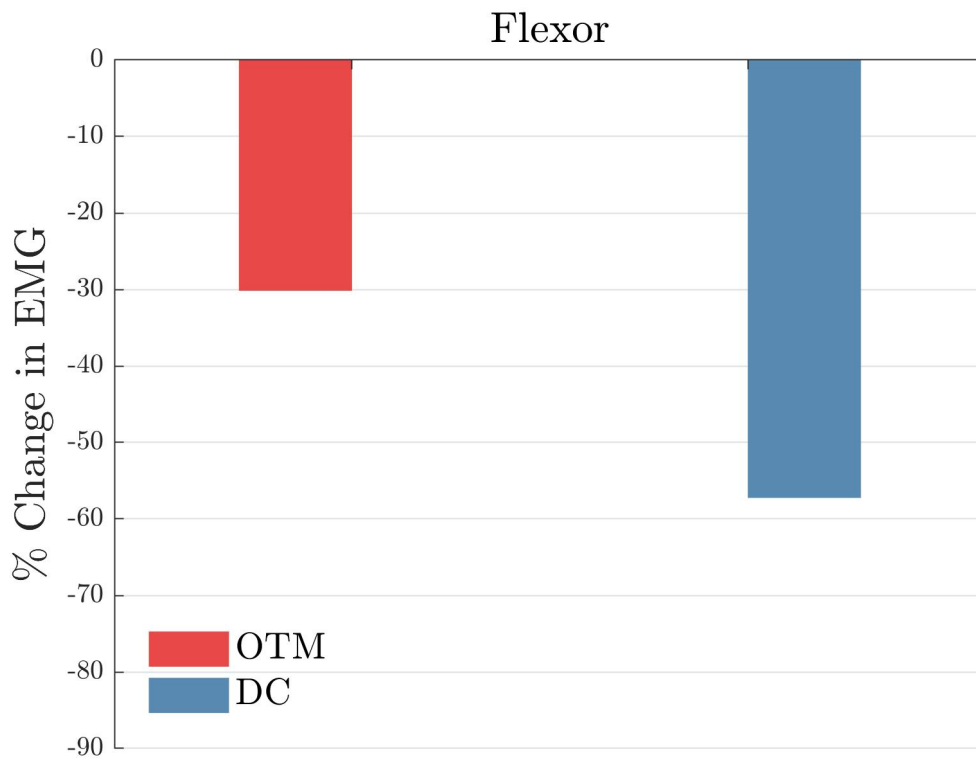


Figure 3.14: Percetual reduction of muscolar activity. In red the signal acquired using the OTM module, in blue using the DC motor prototype, in grey without any assistance

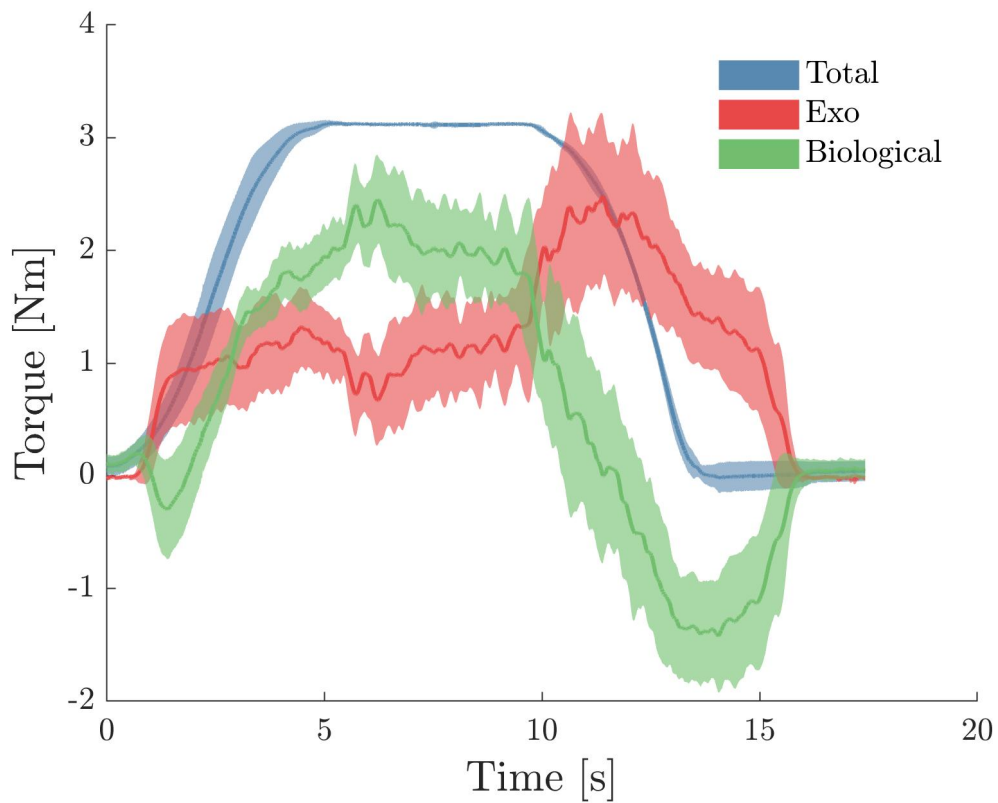


Figure 3.15: Requested torque mean and standard deviation across repetitions: in blue the total torque, in green the biological torque provided by the subject, in red the torque provided by the exosuit

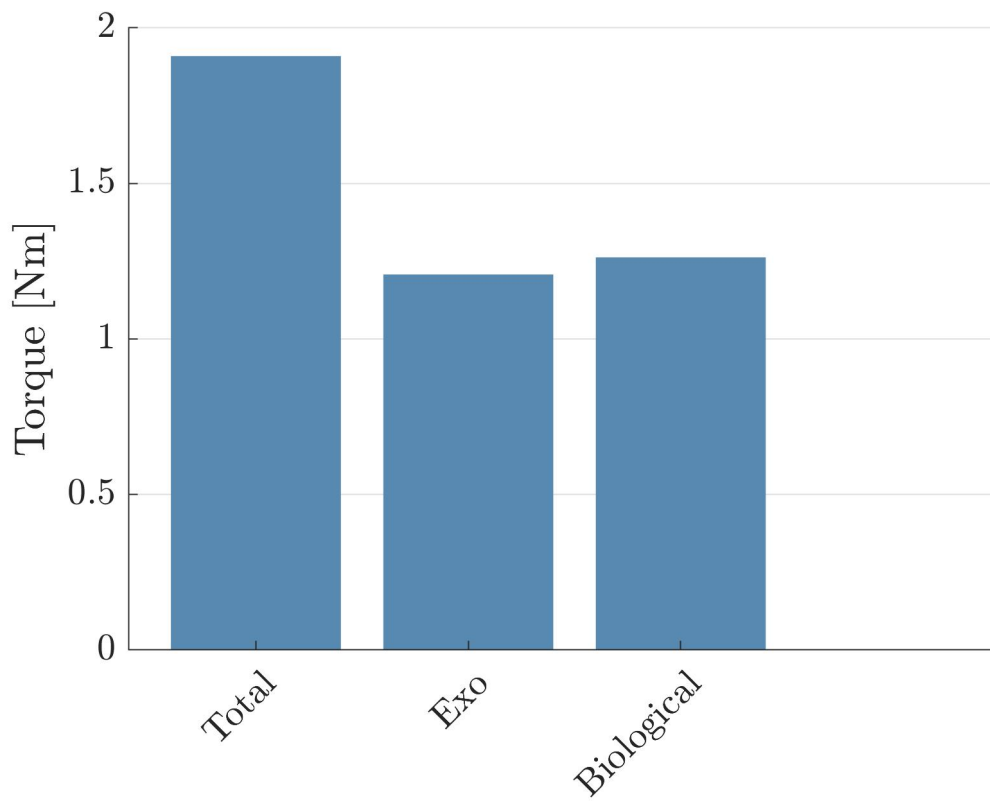


Figure 3.16: Distribution of the total torque between subject and exosuit.

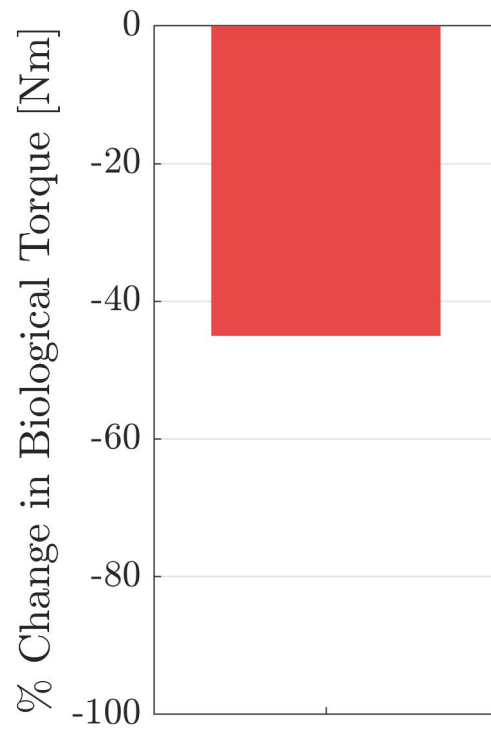


Figure 3.17: Percetual reduction of human effort in terms of torque using the exosuit.

Chapter 4

Discussion and Future Works

In this chapter main results of this project are shown comparing them with the aim and motivations that inspired this work. In the second section it is discussed the effectiveness of the overall design focusing on evaluation of performances. In the last section future works are proposed: focusing on improving the module and investigating other solutions for an OTM system.

4.1 Results

A mechanical upgrade of the module has been proposed, it showed its robustness provided by tests without any load, in loaded conditions and used by a subject. The control algorithm for controlling the module here proposed resulted to be effective and has been characterized. Furthermore, it has been proposed a theoretical approach to understand more accurately the stability of sliding mode regime when it is modulated by an integral stage. Module and control algorithm are been characterized with different kind of tests: showing the error when the input is a ramp, a sinwave, thus, a frequency response was experimentally derived. It has been evaluated the loaded behavior of the module imposing cables' tension.

Connecting the OTM module to the exosuit we evaluated performances when the load is a human subject. To achieve this result an high level control algorithm already existing has been modified in order to provide the correct reference to the module.

Different kind of performances have been evaluated: EMG reduction, torque and trajectory analysis.

4.2 Discussion

The design here described showed many critical issues: an unexpected behavior in the frequency domain, with the appearance of a resonance peak changing the maximum angular velocity. It has been proposed an hypothesis to explain this behavior but further analysis are needed.

The loaded behavior of the module showed a low maximum cable tension that the prototype can provide. This is an important issue that would limit the maximum amount of assistance that the device can deliver.

A particular issue is the torque provided when connected to the exosuit: the controller is too slow to provide the right torque at right time resulting in an undesired and innatural work of the subject that has to oppose a torque to the assistive one. The smoothness of trajectories is really affected by this problem.

4.3 Future works

This work demonstrated the effectiveness of an Uni-Drive system: it is lightweight, low cost and simple to control. On the other hand, many issues rose up. The main problem is to increase the velocity of the control system. In order to reach this result many paths could be followed.

First of all, electromechanical clutches could be substitute with devices of the same type but faster and faster. This solution is not so difficult to be implemented and needs few changes in mechanical design. On the other , in this way it will be always impossible to reach perfectly smooth trajectories. Thus, it is possible to design a module with an Infinite Variable Transmission (IVT). It will need a servo-motor for each DoF that has to move independently but energy and weight cost of this solution is of the same order of using electromagnetic clutches.

Independently from choosing a different design it worths to design a multi Dof system using OTM modules to see which is the weight of an Uni-Drive solution when compared with classical approach in case of similar number of degrees of freedom actuated.

Improvements of the control architecture are possible and future works could focus on many new approaches. In particular, when you are dealing with human-robot interaction it is important to assure robustness performances. To achieve this result an interesting investigation can be performed identifying the plant and its nonlinearities [30].

Concluding it is possible to say that this project not only achieved many interesting results but also proposed a lot of new challenges to face. In my opinion, this is the heart of scientific research: you will never say that you have just reached a new place, always it is your new starting point.

Bibliography

- [1] C. Mathers, D. M. Fat, J. T. Boerma, and World Health Organization., *The global burden of disease : 2004 update*, World Health Organization, 2008.
- [2] R. S. Mosher, *Handyman to Hardiman*, SAE International, Warrendale, PA, SAE Technical Paper 670088, Feb. 1967.
- [3] Russ Angold, James Lubin, Mario Solano, Chris Paretich, Tom Mastaler; Ekso Bionics, Inc., assignee *Exoskeleton and Method of Providing an Assistive Torque to an Arm of a Wearer*, US patent 20170173783, 2017 Jun 22.
- [4] Veneman JF, Kruidhof R, Hekman EEG, Ekkelenkamp R, van Asseldonk EHF, Kooij van der H: *Design and evaluation of the LOPES exoskeleton robot for interactive gait rehabilitation*, IEEE Trans Neural Syst Rehabil Eng. 2007, 15 (3): 379-386.
- [5] P. Polygerinos, Z. Wang, K. C. Galloway, R. J. Wood, and C. J. Walsh, *Soft robotic glove for combined assistance and at-home rehabilitation*, In Rob. Auton. Syst., vol. 73, pp. 135-143, 2015.
- [6] H. In and K.-j. Cho, *Exo-Glove : Soft wearable robot for the hand using soft tendon routing system*, In IEEE Robot. Autom., vol. 22, no. March 2015, pp. 97-105, 2015.
- [7] M. Xiloyannis, L. Cappello, Dinh Binh Khanh, Shih-Cheng Yen, and L. Masia, *Modelling and design of a synergy-based actuator for a tendon-driven soft robotic glove*, In 6th IEEE Int. Conf. Biomed. Robot. Biomechatronics, Jun 2016.
- [8] A. T. Asbeck, K. Schmidt, I. Galiana, D. Wagner, and C. J. Walsh, *Multi-joint Soft Exosuit for Gait Assistance*, IEEE Int. Conf. Robot. Autom., pp. 6197-6204, 2015.
- [9] D. Popov, I. Gaponov, and J.-H. Ryu, *Portable Exoskeleton Glove with Soft Structure for Hand Assistance in Activities of Daily Living*, In IEEE/ASME Trans. Mechatronics, 2016.
- [10] Quinlivan, B. T. and Lee, S. and Malcolm, P. and Rossi, D. M. and Grimmer, M. and Siviy, C. and Karavas, N. and Wagner, D. and Asbeck, A. and Galiana, I. and Walsh, C. J., *Assistance magnitude versus metabolic cost reductions for a tethered multiarticular soft exosuit*, In Sci. Robot. 2-2, 2017.
- [11] F. Panizzolo, I. Galiana, A. T. Asbeck, C. Siviy, K. Schmidt, K. G. Holt,

- and C. J. Walsh, *A biologically-inspired multi-joint soft exosuit that can reduce the energy cost of loaded walking*, J. Neuroeng. Rehabil., vol. submitted, no. 1, p. 43, Jan 2016.
- [12] M. Xiloyannis, L. Cappello, B. Dinh, C. Antuvan, and L. Masia, *Design and Preliminary Testing of a Soft Exosuit for Assisting Elbow Movements and Hand Grasping*, Converging Clin. Eng. Res. Neurorehabilitation II, 2017.
- [13] K. Dinh, L. Cappello, M. Xiloyannis, and L. Masia, *Position Control using Adaptive Backlash Compensation for Bowden Cable Transmission in Soft Wearable Exoskeleton*, Intell. Robot and Syst. (IROS), 2016 IEEE/RSJ, pp. 5670-5676, 2016.
- [14] L. Cappello, D. K. Binh, S. C. Yen, and L. Masia, *Design and preliminary characterization of a soft wearable exoskeleton for upper limb*, Int. Conf. Biomed. Robot. Biomechatronics, pp. 623-630, July 2016.
- [15] T. R. Hunt, C. J. Berthelette, and M. B. Popovic, *Linear One-to-Many (OTM) system: Many degrees of freedom independently actuated by one electric motor*, 5th Annual IEEE International Conference on Technologies for Practical Robot Applications (TePRA), Greater Boston Area, Massachusetts, USA, April 22-23, 2013.
- [16] James Douglass Penn, *A Multiple Degree of Freedom Actuator Using a Single Vibrating Transducer*, Doctor of Philosophy thesis at the Massachusetts Institute of Technology, June 2012.
- [17] Guowu Jia, Guang Chen and Ming Xie, *Design of a novel compact dexterous hand for teleoperation* Proceedings 2001 IEEE International Symposium on Computational Intelligence in Robotics and Automation (Cat. No.01EX515), 2001, pp. 5-10
- [18] N. Tirasuntarakul and A. Dheeravongkit, *Design and Analysis of a Micro Actuating Mechanism Driving Multi-Degree of Freedom*, Applied Mechanics and Materials, Vol. 851, pp. 464-469, 2016
- [19] Shiqi Li, Yang Liu, Ming Xie, (2011) *Implementation of a single motor driven manipulator with multiple joints*, Industrial Robot: An International Journal, Vol. 38 Issue: 1, pp.48-57
- [20] R.A. Skoog and G.L. Blankenship, *Generalized Pulse-Modulated Feedback System: Normas, Gains, Lipschitz Constants, and Stability*, IEEE Transactions on Automatic Control, Vol. AC-15, No. 3, pp. 300-315, June 1970
- [21] H. Sira-Ramirez, *Sliding Regimes In Pulse-Width-Modulation Systems Design*, Proceedings of the 28th IEEE Conference on Decision and Control, Tampa, Florida, FL, 1989, pp.2199-2204 vol. 3.
- [22] H. Sira-Ramirez, *A geometric approach to pulse-width modulated control in nonlinear dynamical systems.*, IEEE Transactions on Automatic Control, 34(2):184—187, February 1989.
- [23] H. Karbasi, *Uni-Drive Modular Robots*, University of Waterloo, 2002.
- [24] M. Canesi, M. Xiloyannis, A. Ajoudani, A. Bicchi and L. Masia, *Modular*

- one-to-many clutchable actuator for a soft elbow exosuit*, 2017 International Conference on Rehabilitation Robotics (ICORR), London, 2017, pp. 1679-1685.
- [25] C. E. Shannon, *Communication in the Presence of Noise*, in Proceedings of the IRE, vol. 37, no. 1, pp. 10-21, Jan. 1949.
- [26] H. J. Hermens, B. Freriks, C. Disselhorst-Klug, and G. Rau, *Development of recommendations for SEMG sensors and sensor placement procedures*, J. Electromyogr. Kinesiol., vol. 10, no. 5, pp. 361–374, 2000.
- [27] D. Chiaradia, M. Xiloyannis, C. W. Antuvan, A. Frisoli, L. Masia, *Design and Embedded Control of a Soft Elbow Exosuit*, 2018 IEEE International Conference on Soft Robotics (RoboSoft), Livorno, 2018.
- [28] H. Karbasi, A. Khajepour, and J. P. Huissoon, *Unidrive modular robot: Dynamics, control, and experiments*, Journal of Dynamic Systems, Measurement and Control, Transactions of the ASME, 128(4):969 - 975, 2006.
- [29] A. S. Kembraum, M. Kitchell and M. Crittenden, *An ultra-compact infinitely variable transmission for robotics*, 2017 IEEE International Conference on Robotics and Automation (ICRA), Singapore, 2017, pp. 1800-1807.
- [30] V. Cerone and D. Regruto, *Parameter bounds for discrete-time Hammerstein models with bounded output errors*, in IEEE Transactions on Automatic Control, vol. 48, no. 10, pp. 1855-1860, Oct. 2003.
- [31] Yu W, Rosen J, Li X. *PID admittance control for an upper limb exoskeleton*. Proc 2011 Am Control Conf. 2011;p. 1124–1129.
- [32] MacKay WA, Crammond DJ, Kwan HC, Murphy JT. *Measurements of human forearm viscoelasticity*. J Biomech. 1986;19(3):231–238.
- [33] Kazerooni H, Racine JL, Huang L, Steger R. *On the control of the Berkeley Lower Extermity Exoskeleton (BLEEX)*. In: Proc. IEEE Int. Conf. Robot. Autom.; 2005. p. 4353–4360.
- [34] Buckley MA, Yardley A, Johnson GR, Cams DA. *Dynamics of the upper limb during performance of the tasks of everyday living: a review of the current knowledge base*. J Eng Med. 1996 jun;210(4):241–247.
- [35] Clancy EA, Morin EL, Merletti R. *Sampling, noise-reduction and amplitude estimation issues in surface electromyography*. In: J. Electromyogr. Kinesiol.. vol. 12; 2002. p. 1–16.

Appendix A

MATLAB codes

A.1 Choosing T_{PWM}

```
load('duty_cycle_effect_n1_50.mat');
duty_cycle_effect=duty_cycle_effect;
Ts=1/1000;
mean_speed=zeros(10,7);
%% connect different files in a position matrix
position(7,:)=duty_cycle_effect(3,1:210001);
%% analysys
for p=1:7
    for a=1:21
        speed(a,:)=diff(position(p,((a-1)*10000+1):(a*10000-1)))/0.001;
        mean_speed(a,p)=mean(speed(a,:));
        rmse_speed(a,p)=sqrt(sum((speed(a,:)-mean_speed(p)).^2)/length(speed));
    end
    % mean_speed(p)=mean(speed(a,:));
    % rmse_speed(p)=sqrt(sum((speed(a,:)-mean_speed(p)).^2)/length(speed));
    x=linspace(-1,1,20);
    theta(1,1)=0;
    v=(-1:0.1:1);
    for i=1:(210000-1)
        j=floor(i/10^4)+1;
        theta(i+1)=-v(j)*15*Ts+theta(i);
        error(i)=theta(i)-position(p,i);
    end
    for j=1:21
        rmse(p)=sqrt(sum(error((j-1)*10000+1:j*10000-1).^2)/10000);
    end
    rmse_tot(p)=sqrt(sum(error.^2)/10000);
    speed_normal(:,p)=mean_speed(:,p)./max(mean_speed(:,p));
```

```

    m=polyfit(v,speed_normal(:,p)',1);
    n=polyval(m,v);
    [r2(p) k(p)]=rsquare(speed_normal(:,p)',n);
%    figure(1), hold on;
%    plot(v,speed_normal(p));

end

f_h = figure(1);
p = plot(v,speed_normal);
l = legend([p],[ 'Tzoh = 0.02, RMSE = ',num2str(rmse_tot(1)),'rad' ],...
    [ 'Tzoh = 0.06, RMSE = ',num2str(rmse_tot(2)),'rad' ],...
    [ 'Tzoh = 0.10, RMSE = ',num2str(rmse_tot(3)),'rad' ],...
    [ 'Tzoh = 0.20, RMSE = ',num2str(rmse_tot(4)),'rad' ],...
    [ 'Tzoh = 0.30, RMSE = ',num2str(rmse_tot(5)),'rad' ],...
    [ 'Tzoh = 0.40, RMSE = ',num2str(rmse_tot(6)),'rad' ],...
    [ 'Tzoh = 0.50, RMSE = ',num2str(rmse_tot(7)),'rad' ]});
set(l,'Interpreter','latex')
grid on
figure (2)
plot(v,rmse)

```

A.2 Trajectory tracking

```

clear all
close all
for j=2:4
load(['rampfollower@',int2str(j),'5.mat']);
T=0.001;
Fs = 1/T;
N=9e3;
for i=0:10
    a=25*Fs*i+1*Fs;
    b=25*Fs*i+15*Fs;
    er_cw=rampfollower(2,a:(a+9*Fs))-rampfollower(3,a:(a+9*Fs));
    er_ccw=rampfollower(2,b:(b+9*Fs))-rampfollower(3,b:(b+9*Fs));
%    delay(j-1,10+i+1)=finddelay(rampfollower(2,a:(a+9*Fs)),rampfollower(3,a:(a+9*Fs)),1);
%    delay(j-1,10-i+1)=finddelay(rampfollower(2,b:(b+9*Fs)),rampfollower(3,b:(b+9*Fs)),1);
    RMSE(j-1,10+i+1)=sqrt(sum(er_cw.^2)/N)*pi/180;
    RMSE(j-1,10-i+1)=sqrt(sum(er_ccw.^2)/N)*pi/180;
    speed_n(10+i+1)=0.1*i;
    speed_n(10-i+1)=-0.1*i;
end
end
% C = linspecer(3,'qualitative');

```

```

% f_h = figure(2); hold on,grid on,
%
% p1 = scatter(speed_n,delay(1,:),20,C(1,:),'filled','MarkerFaceAlpha',.4);
% p2 = scatter(speed_n,delay(2,:),20,C(2,:),'filled','MarkerFaceAlpha',.4);
% p3 = scatter(speed_n,delay(3,:),20,C(3,:),'filled','MarkerFaceAlpha',.4);
%
% l = legend({'$\omega = 25$ rad/s$' },...
%           ['$\omega = 35$ rad/s$' ],...
%           ['$\omega = 45$ rad/s$' ],...
%           },'Location','NorthWest');
% %set(gca,'TickLabelInterpreter','Latex');
% set(l,'box','off','FontSize',12);
% set(l,'Interpreter','latex');
% box off; set(gcf,'Color',[1,1,1]);
%
% xlabel('$v/v_{max}$', 'Interpreter','latex','FontSize',20)
% ylabel('Delay $[s]$', 'Interpreter','latex','FontSize',20)
% axis([-1 1 0 15])
% print('Load','-r600','-djpeg')
%
% % axis([-7000 7000 -1 1])
C = linspace(3,'qualitative');
f_h = figure(1); hold on,grid on,

p1 = scatter(speed_n,RMSE(1,:),20,C(1,:),'filled','MarkerFaceAlpha',1);
p2 = scatter(speed_n,RMSE(2,:),20,C(2,:),'filled','MarkerFaceAlpha',1);
p3 = scatter(speed_n,RMSE(3,:),20,C(3,:),'filled','MarkerFaceAlpha',1);

l = legend({'$\omega = 25$ rad/s$' },...
           ['$\omega = 35$ rad/s$' ],...
           ['$\omega = 45$ rad/s$' ],...
           },'Location','NorthWest');
%set(gca,'TickLabelInterpreter','Latex');
set(l,'box','off','FontSize',12);
set(l,'Interpreter','latex');
box off; set(gcf,'Color',[1,1,1]);

xlabel('$\omega/\omega_{max}$', 'Interpreter','latex','FontSize',20)
ylabel('RMSE $[rad]$', 'Interpreter','latex','FontSize',20)
%axis([-1 1 0 15])
print('Load','-r600','-djpeg')

C = linspace(2,'qualitative');
f_h = figure(2); hold on,grid on,
time=rampfollower(1,25500:27500);
p1 = plot(time-25.5, rampfollower(2,25500:27500)*180/pi,'Color',C(1,:),'LineWidth',2);

```

```

p2 = plot(time-25.5,rampfollower(3,25500:27500)*180/pi,'Color',C(2,:), 'LineWidth',2);
%p3 = scatter(speed_n,RMSE(3,:),20,C(3,:), 'filled', 'MarkerFaceAlpha',1);

l = legend({'Output' ],...
          ['Reference' ],...
          ['$\omega = 45 \text{ rad/s}$' ],...
          }, 'Location', 'NorthWest');
%set(gca, 'TickLabelInterpreter', 'Latex');
set(l, 'box', 'off', 'FontSize', 12);
set(l, 'Interpreter', 'latex');
box off; set(gcf, 'Color', [1,1,1]);

xlabel('Time [s]', 'Interpreter', 'latex', 'FontSize', 20)
ylabel('$\theta$ [deg]', 'Interpreter', 'latex', 'FontSize', 20)
axis([0 2 0 360])
print('data', '-r600', '-djpeg')
% axis([-7000 7000 -1 1])

```

A.3 Bandwidth

```

% clear all
% close all
C = linspecer(4, 'qualitative');
for j=2:5
load(['sweep@', int2str(j), '.mat']);
T=0.001;
Fs = 1/T;
L=20e3;
n=2^nextpow2(20e3-2e3);
N=floor(length(sweep)/L);
%j=1;
for i=1:(N-1)
    w(j,i)=sweep(4,L*i+1);
    Y=fft(sweep(2:3, (L*i+1+2e3):(L*i+L-1)),n,2);
    [r,k]=max(Y(2,:));
    z = 1/(r/Y(1,k));
    Mag(j,i)=(abs(z));
    % Pha(i)=angle(z)*180/2/pi;
    Pha(j,i)=-abs(angle(z)*180/2/pi);
end

f_h = figure(1); hold on,
subplot(2,1,1)
m(j-1)= scatter(w(j,:),mag2db(Mag(j,:)),20,C(j-1,:), 'filled', 'MarkerFaceAlpha',.4);
set(gca, 'XScale', 'log')

```

```

set(gca,'TickLabelInterpreter','Latex');
grid on, hold on
box off; set(gcf,'Color',[1,1,1]);

%xlabel('Frequency [Hz]', 'Interpreter','latex','FontSize',20)
ylabel('Mag [dB]', 'Interpreter','latex','FontSize',20)
%axis([1e-2 100 -10 3])
print('Load','-r600','-djpeg')
l = legend({'$\omega = 25$ rad/s$' },...
    ['$\omega = 35$ rad/s$' ],...
    ['$\omega = 45$ rad/s$' ],...
    ['$\omega = 55$ rad/s$' ],...
    },'Location','NorthEast');
set(l,'box','off','FontSize',12);
set(l,'Interpreter','latex');

subplot(2,1,2)
p(j-1) = scatter(w(j,:),Pha(j,:),20,C(j-1:,:),'filled','MarkerFaceAlpha',.4);
set(gca, 'XScale', 'log')
set(gca,'TickLabelInterpreter','Latex');
grid on,
box off; set(gcf,'Color',[1,1,1]);

xlabel('Frequency [Hz]', 'Interpreter','latex','FontSize',20)
ylabel('Pha[deg]', 'Interpreter','latex','FontSize',20)
axis([1e-2 100 -120 0])
print('Load','-r600','-djpeg')
set(gca, 'XScale', 'log')
set(gca,'TickLabelInterpreter','Latex');
grid on
hold on
% P2 = abs(Y/n);
% P1 = P2(:,1:n/2+1);
% P1(:,2:end-1) = 2*P1(:,2:end-1);
% figure;plot(P1(1,1:n/2))
% hold on;plot(P1(2,1:n/2),'r')

end
time=sweep(1,140000:160000);
C = linspecer(2,'qualitative');
figure(2),
p1 = plot(time-140,sweep(2,140000:160000),'Color',C(1,:), 'LineWidth',2);
hold on
p2 = plot(time-140,sweep(3,140000:160000),'Color',C(2,:), 'LineWidth',2);
%set(gca, 'XScale', 'log')
set(gca,'TickLabelInterpreter','Latex');

```

```
grid off,
box off; set(gcf,'Color',[1,1,1]);

xlabel('Time [s]', 'Interpreter','latex','FontSize',20)
ylabel('\theta[rad]', 'Interpreter','latex','FontSize',20)
l = legend({'Output' },...
    ['Reference' ]});
set(l,'box','off','FontSize',12);
set(l,'Interpreter','latex');
axis([0 20 -5 8])
print('data','-r600','-djpeg')
%set(gca, 'XScale', 'log')
set(gca,'TickLabelInterpreter','Latex');
```

A.4 Load behavior

```
clear all
close all

T=1e-3;
Fs = 1/T;
for j=1:5
    load(['load',int2str(j),'.mat']);
for i=0:9
    a=15*Fs*i+1;
    b=a+15*Fs;
    if(i==9) er_cw=sweep(2,a:(floor(b/2)))-sweep(3,a:(floor(b/2)));
    else er_cw=sweep(2,a:b)-sweep(3,a:b); end
    RMSE(j,i+1)=sqrt(sum(er_cw.^2)/length(er_cw));
    tau(i+1)=sweep(4,a+100);
end
end
tension=tau/(41e-3/2);
C = linspecer(1,'qualitative');
f_h = figure(1); hold on,grid on,
RMSE_mean=mean(RMSE);

p1 = scatter(tension,RMSE(1,:),20,C(1:),'filled','MarkerFaceAlpha',0.2);
p2 = scatter(tension,RMSE(2,:),20,C(1:),'filled','MarkerFaceAlpha',0.2);
p3 = scatter(tension,RMSE(3,:),20,C(1:),'filled','MarkerFaceAlpha',0.2);
p4 = scatter(tension,RMSE(4,:),20,C(1:),'filled','MarkerFaceAlpha',0.2);
p5 = scatter(tension,RMSE(5,:),20,C(1:),'filled','MarkerFaceAlpha',0.2);
p6 = scatter(tension,RMSE_mean,20,C(1:),'filled','MarkerFaceAlpha',1);
% l = legend({'\omega = 25 rad/s' },...
```

```

%     ['$\omega = 35 rad/s$' ],...
%     ['$\omega = 45 rad/s$' ],...
%     },'Location','NorthWest');
set(gca,'TickLabelInterpreter','Latex');
% set(1,'box','off','FontSize',12);
% set(1,'Interpreter','latex');
box off; set(gcf,'Color',[1,1,1]);

xlabel('Cable Tension $[N]$', 'Interpreter','latex','FontSize',20)
ylabel('RMSE $[rad]$', 'Interpreter','latex','FontSize',20)
%axis([-1 1 0 15])
print('Load','-r600','-djpeg')

% axis([-7000 7000 -1 1])

```

A.5 Test on subject

```

%%
cd C:\Users\aeqi\Google' Drive\Eugenio\exp\euge\euge\exp_permichele\exo\
clear all; close all; clc;

C = linspecer(3,'qualitative');
fs = 1e3;
wo_color = [200 200 200]./255;
w_color = [0 0 0]/255;
ref_color = C(3,:);
% idx = [1.35e5:1.94e5];%last 3 contractions

ME = {'notempty'};
while(~isempty(ME))
    %choose analysis
    prompt = 'Choose analysis:\n 1-Muscles \n 2-Torques \n 3-Trajectoris \n';
    analysis = input(prompt);

    if(analysis == 1)
%% 1 EMG Analysis
%----- 1 Preprocessing -----
% Use the e_cal a functions to calibrate the filters
% described in Merletti et al. (noise filtering, whitening, demodulation,
% smoothening and linearisation, demod and lin of 2nd order for dynamic
% and 1st order for isometric).
%----- 2 Remove outliers -----
% Remove spikes of EMG data using a symmetric threshold of 12 SD
%----- 3 Extract amplitude -----
% Use e_amp to extract amplitude noise filtering, whitening, demodulation,

```

```
% smoothing and linearisation, demod and lin of 2nd order for dynamic
% and 1st order for isometric).
%----- 4 Segmentation -----
% Extract epochs of interest: for the dynamic task use data with elbow
% angle above 10deg, for isometric find the indexes when the joint is at
% its max position, remove first and last second.
%----- 5 Extract feature -----
% Calculate the Average rectified value for the isometric and the RMS for
% the dynamic task.
    folder = dir('*wo');
    cd(folder.name)

    load MVC_segmented;
    EMGinfo_flex_wo = e_cal(flex(:,2), 1, flex_rest(:,2), fs, 'SmoothFixWin', 800);
    EMGinfo_flex_wo.DemodM = 2; %RMS

    EMGinfo_ext_wo = e_cal(ext(:,2), 1, ext_rest(:,2), fs, 'SmoothFixWin', 800);
    EMGinfo_ext_wo.DemodM = 2; %RMS

    cd ../

    folder = dir('*w');
    cd(folder.name)

    load MVC_segmented;
    EMGinfo_flex_w = e_cal(flex(:,2), 1, flex_rest(:,2), fs, 'SmoothFixWin', 800);
    EMGinfo_flex_w.DemodM = 2; %RMS

    EMGinfo_ext_w = e_cal(ext(:,2), 1, ext_rest(:,2), fs, 'SmoothFixWin', 800);
    EMGinfo_ext_w.DemodM = 2; %RMS

    cd ../

    folder = dir('*DC');
    cd(folder.name)

    load MVC_segmented;
    EMGinfo_flex_DC = e_cal(flex(:,2), 1, flex_rest(:,2), fs, 'SmoothFixWin', 800);
    EMGinfo_flex_DC.DemodM = 2; %RMS

    EMGinfo_ext_DC = e_cal(ext(:,2), 1, ext_rest(:,2), fs, 'SmoothFixWin', 800);
    EMGinfo_ext_DC.DemodM = 2; %RMS

    cd ../

    %extract amplitude
```

```

load Re_Data;
Muscles = Muscles-mean(Muscles);%make sure they are symmetric around 0

raw = Muscles(:,[2:3,5:6,8:9]);
time = [1:length(raw)]/fs;
idx = [60e3:length(Muscles)];%remove first 3 movements1

% plot muscles
figure, hold on;box off; set(gcf,'Color',[1,1,1]);
h_p = plot(time,raw(:,[1,3,5]), 'LineWidth', 1.5);
set(gca,'FontSize',12);
set(h_p(1),'Color',wo_color);
set(h_p(2),'Color',C(2,:));
set(h_p(3),'Color',C(1,:));

grid on; xlabel('Time [s]', 'Interpreter','latex','FontSize',16)
ylabel('Raw EMG [V]', 'Interpreter','latex','FontSize',16)
h_leg= legend([h_p(1),h_p(2),h_p(3)],{'W/O Exo',...
    'W/ Exo - OTM','W/ Exo - DC'},...
    'Location','NorthWest');
set(h_leg,'box','off','FontSize',14)
set(h_leg,'Interpreter','latex')
grid off; set(gca,'TickLabelInterpreter','Latex');
axis([0 time(end) -1.2 1.7 ])
% cd C:\Users\Michele\Xiloyannis\Dropbox\Conferences_Papers\InPreparation\JNER\
% print('Raw_EMG','-r300','-dsvg')
print('Raw_EMG','-r300','-djpeg')
% cd C:\Users\Michele\Xiloyannis\Dropbox\Michele\Elbow\Exp\Subjects\Subj1\Fatig

muscles_wo = Muscles(:,2:3);
muscles_w = Muscles(:,5:6);
muscles_DC = Muscles(:,8:9);

%Remove "outliers"
muscles_wo(abs(muscles_wo)>8*std(muscles_wo)) = 0;
muscles_w(abs(muscles_w)>8*std(muscles_w)) = 0;
muscles_DC(abs(muscles_DC)>8*std(muscles_DC)) = 0;

%Extract amplitude - flexor
amp_flex_wo= e_amp(muscles_wo(:,1),EMGinfo_flex_wo);
amp_flex_w = e_amp(muscles_w(:,1),EMGinfo_flex_w);
amp_flex_DC = e_amp(muscles_DC(:,1),EMGinfo_flex_DC);

%Extract amplitude - extensor
amp_ext_wo = e_amp(muscles_wo(:,2),EMGinfo_ext_wo);
amp_ext_w = e_amp(muscles_w(:,2),EMGinfo_ext_w);

```

```

amp_ext_DC = e_amp(muscles_DC(:,2),EMGinfo_ext_DC);

kinematics = Traj(1:end-1,[4,5,10,15]);

%calculate RMS over the contractions
%flexor
rms_flex = [rms(amp_flex_wo(idx)),rms(amp_flex_w(idx))];
rms_delta = rms_flex(2) - rms_flex(1);
rms_ratio = (rms_flex(2) - rms_flex(1))/rms_flex(1)*100;

rms_flex_DC = [rms(amp_flex_wo(idx)),rms(amp_flex_DC(idx))];
rms_delta_DC = rms_flex_DC(2) - rms_flex_DC(1);
rms_ratio_DC = (rms_flex_DC(2) - rms_flex_DC(1))/rms_flex_DC(1)*100;

%extensor
rms_ext = [rms(amp_ext_wo(idx)),rms(amp_ext_w(idx))];
rms_delta_ext = rms_ext(2) - rms_ext(1);
rms_ratio_ext = (rms_ext(2) - rms_ext(1))/rms_ext(1)*100;

rms_ext_DC = [rms(amp_ext_wo(idx)),rms(amp_ext_DC(idx))];
rms_delta_DC_ext = rms_ext_DC(2) - rms_ext_DC(1);
rms_ratio_DC_ext = (rms_ext_DC(2) - rms_ext_DC(1))/rms_ext_DC(1)*100;

%plot
figure, set(gcf,'Color',[1,1,1]);
h1 = plot(time,amp_flex_wo); hold on, h2 = plot(time,amp_flex_w);
h3 = plot(time,amp_flex_DC);

set(gca,'FontSize',12);
set(h1,'Color',wo_color,'LineWidth',1.5);
set(h2,'Color',C(2,:), 'LineWidth',1.5);
set(h3,'Color',C(1,:), 'LineWidth',1.5);

h_leg= legend([h1,h2,h3],{'W/O Exo',...
    'W/ Exo - OTM','W/ Exo - DC'},...
    'Location','NorthEast');
set(h_leg,'box','off','FontSize',14)
set(h_leg,'Interpreter','latex'),box off;
xlabel('Time [s]', 'Interpreter','latex','FontSize',16)
ylabel('EMG Envelope [V]', 'Interpreter','latex','FontSize',16)
grid off; set(gca,'TickLabelInterpreter','Latex');
print('emg_env','-r300','-djpeg')
%% plot trajectory and raw flexors and extensors for comparison
idx = [1:length(Muscles)];
time_idx = [0:length(idx)-1]/fs;

```

```

%trajectory
figure, hold on;box off; set(gcf,'Color',[1,1,1]);
h_p_wo = plot(time_idx,Traj(idx,[5,10,15]), 'LineWidth', 2);
set(gca,'FontSize',12);
set(h_p_wo(1),'Color',wo_color);
set(h_p_wo(2),'Color',[C(2,:),.6]);
set(h_p_wo(3),'Color',[C(1,:),.6]);

xlabel('Time [s]', 'Interpreter','latex','FontSize',16)
ylabel('Joint Angle [deg]', 'Interpreter','latex','FontSize',16)
grid off; set(gca,'TickLabelInterpreter','Latex');
set(gca,'YTick',[0 30 60 90 120],'YTickLabel',{'0','30','60','90','120'},'XTickLa
axis([0 time_idx(end) -10 120 ])
h_leg= legend([h_p_wo],{'W/O Exo',...
    'W/ Exo - OTM','W/ Exo - DC'},...
    'Location','NorthWest');
set(h_leg,'box','off','FontSize',14)
set(h_leg,'Interpreter','latex')
alpha(.6)
% pbaspect([6 1 1])
% cd C:\Users\Michele\Xiloyannis\Dropbox\Conferences_Papers\InPreparation\JNER\
% name = ['traj_mus',num2str(subject)];
% print(name,'-r300','-dsvg')
print('traj','-r300','-djpeg')
% cd C:\Users\Michele\Xiloyannis\Dropbox\Michele\Elbow\Exp\Subjects\Subj1\Testi

%% Bar plots of net and % reduction in muscle activity
%flexor
figure, [hBar] = bar([1,2],[rms_ratio,0;0,rms_ratio_DC]);
box off; set(gcf,'Color',[1,1,1]);
set(hBar(1),'FaceColor',C(2:,:), 'EdgeColor','none')
set(hBar(1),'BarWidth',1)

set(hBar(2),'FaceColor',C(1:,:), 'EdgeColor','none')
set(hBar(2),'BarWidth',1)

set(gca,'TickLabelInterpreter','Latex')
set(gca, 'XAxisLocation', 'top')
set(gca,'XTick',[1,2],'XTickLabel',{'',''},'XTickLabelRotation',45);
ylabel('\% Change in EMG','Interpreter','latex', 'FontSize',16)
title('Flexor','Interpreter','latex', 'FontSize',16);
box off; set(gcf,'Color',[1,1,1]);
ax = gca;
ax.XLim = [0.400 2.6000];

```

```

ax.YLim = [-90 0];
ax.YGrid = 'on';
h_leg= legend([hBar(1),hBar(2)],{'OTM',...
    'DC'},...
    'Location','SouthWest');
set(h_leg,'box','off','FontSize',14)
set(h_leg,'Interpreter','latex')

% pbaspect([1 2 1])
% cd C:\Users\Michele\Xiloyannis\Dropbox\Conferences_Papers\InPreparation\JNER\
% name = ['RMS_red_rep',num2str(subject)];
% print(name,'-r300','-dsvg')
    print('change','-r300','-djpeg')
% cd C:\Users\Michele\Xiloyannis\Dropbox\Michele\Elbow\Exp\Subjects\Subj1\Fatig

%extensor
% figure, [hBar] = bar([1,2],[rms_ratio_ext,0;0,rms_ratio_DC_ext]);
% box off; set(gcf,'Color',[1,1,1]);
% set(hBar(1),'FaceColor',C(2,:), 'EdgeColor','none')
% set(hBar(1),'BarWidth',1)
%
% set(hBar(2),'FaceColor',C(1,:), 'EdgeColor','none')
% set(hBar(2),'BarWidth',1)
%
% set(gca,'TickLabelInterpreter','Latex')
% set(gca,'XAxisLocation','top')
% set(gca,'XTick',[1,2],'XTickLabel',{'',''},'XTickLabelRotation',45);
% ylabel('\% Change in EMG','Interpreter','latex','FontSize',16)
% title('Extensor','Interpreter','latex','FontSize',16);
% box off; set(gcf,'Color',[1,1,1]);
% ax = gca;
% ax.XLim = [0.400 2.6000];
% ax.YLim = [0 130];
% ax.YGrid = 'on';
% h_leg= legend([hBar(1),hBar(2)],{'OTM',...
%     'DC'},...
%     'Location','NorthWest');
% set(h_leg,'box','off','FontSize',14)
% set(h_leg,'Interpreter','latex')

% cd C:\Users\Michele\Xiloyannis\Dropbox\Conferences_Papers\InPreparation\JNER\
% name = ['RMS_red_rep_ext',num2str(subject)];
% print(name,'-r300','-dsvg')
    print('emg_red','-r300','-djpeg')

```

```

% cd C:\Users\Michele\Xiloyannis\Dropbox\Michele\Elbow\Exp\Subjects\Subj1\Fatig

distFig();
ME = {};

elseif(analysis == 2)
    %% 2 Torque analysis

    fs = 1e3;
    H = 1.78;%m
    M = 77;%kg
    m_ext = 0;%1kg weight for the dynamic task
    %ratios from Drillis Table 1
    m = M*0.036;
    l = H*0.273;
    be = 0.2; % from
    lc = 0.4*l;
    %use the same ones as in the model
    w = 0.11;
    b = 0.1;
    ass_level = 1;%value between 0-1, it has to be the same used for the simulink mod

    load Re_Data.mat;

    ordr = 2;
    cut_off_low = 50;
    pass_lvl = 'low';
    %filter trajectories and tension
    theta_wo = f_butterworth_filter(ordr, cut_off_low, fs, pass_lvl,Traj(:,5));
    theta_w = f_butterworth_filter(ordr, cut_off_low, fs, pass_lvl,Traj(:,end));
    f_w = f_butterworth_filter(ordr, cut_off_low, fs, pass_lvl,Traj(:,7));

    %dynamics
    tau_wo = ElbowDyn(m,m_ext,l,be,lc,theta_wo,fs)*ass_level;
    tau_w = ElbowDyn(m,m_ext,l,be,lc,theta_w,fs)*ass_level;
    %assistive torque
    tau_exo = Tension2AssTorque(theta_w,f_w,w,b);
    %human
    tau_h = tau_w - tau_exo;

    % figure, hold on, plot(tau_w), plot(tau_exo), plot(tau_h)

```

```

kinematics = Traj(1:end-1,[4,5,9,10]); %ref, without, with
dummy_indexes = find(kinematics(1:end-1,3) > 1.5); %find movements
changeoint = find(diff(dummy_indexes) > 1);
window = 3e3;
idx = [];
for j = 1:length(changeoint)
    if (j == 1)
        idx(:,j) = [dummy_indexes(1:changeoint(j)); dummy_indexes(changeoint(j)
    else
        idx(:,j) = [dummy_indexes(changeoint(j-1)+1:changeoint(j)); dummy_index
    end
end
% and the last one
idx(:,length(changeoint)+1) = [dummy_indexes(changeoint(end)+1:end); dummy_index

%segment
tau_w_seg = tau_w(idx);
tau_exo_seg = tau_exo(idx);
tau_h_seg = tau_h(idx);

%mean over
tau_w_mean = mean(tau_w_seg,2);
tau_exo_mean = mean(tau_exo_seg,2);
tau_h_mean = mean(tau_h_seg,2);
%std
tau_w_std = std(tau_w_seg,1,2);
tau_exo_std = std(tau_exo_seg,1,2);
tau_h_std = std(tau_h_seg,1,2);

%plot
figure, hold on, box off; set(gcf,'Color',[1,1,1]);
time_l = [1:length(tau_w_mean)]/fs;
f_linear_w = [tau_w_mean+tau_w_std; flipdim(tau_w_mean-tau_w_std,1)];
f_time = [time_l, flipdim(time_l,2)]';
h_fill_w = fill(f_time, f_linear_w, C(1,:));
hold on, plot(time_l, tau_w_mean,'Linewidth',1.5,'Color',C(1,:));
h_fill_w.FaceAlpha = .6;
h_fill_w.EdgeColor = 'none';

%exo
time_l = [1:length(tau_exo_mean)]/fs;
f_linear_exo = [tau_exo_mean+tau_exo_std; flipdim(tau_exo_mean-tau_exo_std,1)];
f_time = [time_l, flipdim(time_l,2)]';
h_fill_exo = fill(f_time, f_linear_exo, C(2,:));
hold on, plot(time_l, tau_exo_mean,'Linewidth',1.5,'Color',C(2,:));

```

```

h_fill_exo.FaceAlpha = .6;
h_fill_exo.EdgeColor = 'none';

%biological
time_l = [1:length(tau_h_mean)]/fs;
f_linear_h = [tau_h_mean+tau_h_std; flipdim(tau_h_mean-tau_h_std,1)];
f_time = [time_l, flipdim(time_l,2)]';
h_fill_h = fill(f_time, f_linear_h, C(3,:));
hold on, plot(time_l, tau_h_mean,'Linewidth',1.5,'Color',C(3,:));
h_fill_h.FaceAlpha = .6;
h_fill_h.EdgeColor = 'none';
box off; set(gcf,'Color',[1,1,1]);

set(gca,'YTick',[-2:1:4])
set(gca,'TickLabelInterpreter','Latex')
set(gca,'FontSize',12);
xlabel('Time [s]','Interpreter','latex','FontSize',16)
box off; set(gcf,'Color',[1,1,1]);
ylabel('Torque [Nm]','Interpreter','latex','FontSize',16)

h_leg = legend([h_fill_w,h_fill_exo,h_fill_h],{'Total','Exo','Biological'},'Location','best','box','off','FontSize',12)
set(h_leg,'Interpreter','latex')

% axis([0 14 -1 8.5])
% pbaspect([4,1,1])
% cd C:\Users\Michele\Xiloyannis\Dropbox\Conferences_Papers\InPreparation\J
% print(name,'-r300','-dsvg')
% print('torque1','-r300','-djpeg')
% cd C:\Users\Michele\Xiloyannis\Dropbox\Michele\Elbow\Exp\Subjects\Subj1\F

%% extract mean from data with elbow angle > 1.5deg
kinematics = Traj(1:end-1,[4,5,9,10]); %ref, without the last -1
dummy_indexes_wo = find(abs(kinematics(1:end-1,2)) > 1.5); %find movements, 2.5deg
dummy_indexes_w = find(abs(kinematics(1:end-1,4)) > 1.5); %find movements, 2.5deg

mean_tau_wo = mean(tau_wo(dummy_indexes_wo,:));

mean_tau_w = mean(tau_w(dummy_indexes_w,:));
mean_tau_exo = mean(tau_exo(dummy_indexes_w,:));
mean_tau_h = mean(abs(tau_h(dummy_indexes_w,:)));%<----- note the absolute value

%% Net Torque
figure, [hBar] = bar([mean_tau_w;mean_tau_exo;mean_tau_h]');

```

```

box off; set(gcf,'Color',[1,1,1]);
set(hBar(1),'FaceColor',C(1,:), 'EdgeColor','none')
set(hBar(1),'BarWidth',.8);
%
%   set(hBar(2),'FaceColor',C(2,:), 'EdgeColor','none')
%   set(hBar(2),'BarWidth',.8);
%
%   set(hBar(3),'FaceColor',C(3,:), 'EdgeColor','none')
%   set(hBar(3),'BarWidth',.8);

set(gca,'TickLabelInterpreter','Latex')
set(gca,'XTick',[1,2,3], 'XTickLabel',{'Total','Exo','Biological'}, 'XTickLabelRotation',45, 'FontSize',14);
ylabel('Torque [Nm]', 'Interpreter','latex', 'FontSize',16)
box off; set(gcf,'Color',[1,1,1]);
ax = gca;
ax.XLim = [0.400 4.5];
ax.YGrid = 'on';

% cd C:\Users\Michele\Xiloyannis\Dropbox\Conferences_Papers\InPreparation\JNER\
% name = ['Tau_rep_subject_', num2str(subject)];
% print(name, '-r300', '-dsvg')
% print('torque2', '-r300', '-djpeg')
% cd C:\Users\Michele\Xiloyannis\Dropbox\Michele\Elbow\Exp\Subjects\Subj1\Fatig

%reduction in biological torque
reduction = (mean_tau_h-mean_tau_wo)./mean_tau_wo*100;
figure, hBar = bar([1],reduction');
box off; set(gcf,'Color',[1,1,1]);
set(hBar(1),'FaceColor',C(2,:), 'EdgeColor','none')
set(hBar(1),'BarWidth',.8);

set(gca,'TickLabelInterpreter','Latex')
set(gca,'XTick',1, 'XTickLabel',{''}, 'XTickLabelRotation',45, 'FontSize',14);
ylabel('\% Change in Biological Torque [Nm]', 'Interpreter','latex', 'FontSize',16)
box off; set(gcf,'Color',[1,1,1]);
ax = gca;
ax.XLim = [0.400 1.6];
ax.YLim = [-100 0];
ax.YGrid = 'on';
set(h_leg,'box','off', 'FontSize',12)
set(h_leg,'Interpreter','latex')
pbaspect([1 2 1])
% cd C:\Users\Michele\Xiloyannis\Dropbox\Conferences_Papers\InPreparation\JNER\
% str = ['Tau_red_subject_', num2str(subject)];
% print(str, '-r300', '-dsvg')
% print('torque_red', '-r300', '-djpeg')

```

```
% cd C:\Users\Michele\Xiloyannis\Dropbox\Michele\Elbow\Exp\Subjects\Subj1\Fatig
%distFig();
ME = {};

elseif(analysis == 3)

    ME = {};

else
    warning('Option not available, select one of the options below:')
end
end
end
```